Organo-aluminum complexation as a dominant metal control on soil carbon storage in Andisols: Global evidence across pedogenic and pH gradients

Kida, Morimaru
Nagano, Hirohiko
Shimada, Hiroaki
Fukumasu, Jumpei
Wagai, Rota

(Citation)
Geoderma,467:117740

(Issue Date)
2026-03

(Resource Type)
journal article

(Version)
Version of Record

Geoderma 467 (2026) 117740

Contents lists available at ScienceDirect

Geoderma

journal homepage: www.elsevier.com/locate/geoderma

Organo-aluminum complexation as a dominant metal control on soil carbon storage in Andisols: Global evidence across pedogenic and pH gradients

Morimaru Kida [a,*], Hirohiko Nagano [b], Hiroaki Shimada [c,1], Jumpei Fukumasu [c], Rota Wagai [c,*]

[a] Soil Science Laboratory, Graduate School of Agricultural Science, Kobe University, 1-1 Rokkodai, Nada, Kobe, Hyogo 657-8501, Japan
[b] Institute of Science and Technology, Niigata University, Niigata 950-2181, Japan
[c] Institute for Agro-Environmental Sciences, National Agriculture and Food Research Organization, Tsukuba, Ibaraki 305-8604, Japan

ARTICLE INFO

Handling Editor: Dr Cornelia Rumpel

Keywords:
Organo-metal complex
Short-range-order minerals
Poorly-crystalline minerals
Organo-mineral interaction
Soil organic matter
Volcanic ash soil
Pedogenesis

ABSTRACT

Soil organic carbon (SOC) storage and persistence are strongly controlled by reactive metal phases, particularly organically complexed aluminum (Al) and iron (Fe) and short-range-order (SRO) minerals. However, their global relevance and the specific metal phases involved remain uncertain due to substantial variability in parent material, soil age, and rock-climate-SOC interactions. Andisols, derived from volcaniclastic materials and enriched in SOC and reactive metals, provide an ideal system to assess metal-SOC associations across broad pedogenic gradients. We compiled a global Andisol database of over 2850 soil samples across 34 countries, covering wide ranges of mean annual temperature (−2 °C to 30 °C), precipitation (60–6000 mm y^{-1}), and soil pH in water (3.1–9.3). Most samples clustered within pH 4.5–6.5, corresponding to an Al-buffered domain where soil pH is predominantly regulated by Al hydrolysis reactions and equilibria among reactive Al pools. Generalized additive mixed model analyses identified organically complexed Al (pyrophosphate-extractable Al, Al_p) as the strongest global predictor of SOC (relative importance = 40%) after accounting for soil depth. SRO Al minerals (acid oxalate-extractable Al minus Al_p) showed moderate importance (relative importance = 10%), whereas reactive Fe and clay content had minor effects. Exchangeable calcium contributed significantly only at pH > ~6.3, consistent with a transition toward base-cation buffering. The persistence of strong SOC-Al_p relationships within the Al-buffered domain, together with consistent pH-dependent shifts in reactive Al and Fe pools, suggests that complexation with pedogenic Al released through weathering may exert a first-order control on mineral-protected SOC beyond Andisols and provides a mechanistic basis for incorporation into global-scale models. Identifying dominant stabilization mechanisms remains critical for determining whether SOC persistence is primarily regulated by carbon inputs, metal supply, or their combined effects. Given its integration of organically complexed and SRO Al phases and its broad data availability, acid oxalate-extractable Al emerges as the most practical proxy for mineral-protected SOC at the global scale.

1. Introduction

Identifying the factors that influence soil organic carbon (SOC) storage is crucial to better understand the stability and response of SOC to changing climate. The stability of SOC is largely dependent on the molecular composition of organic matter and its interactions with soil minerals (Baldock and Skjemstad, 2000; Sollins et al., 1996). While chemical recalcitrance often plays a dominant role in the initial stage of organic matter decomposition, physico-chemical protection provided by soil minerals becomes more relevant for time scales of decades to millennia (Basile-Doelsch et al., 2020; Heckman et al., 2021; Lavallee et al., 2020; Schmidt et al., 2011). The content of clay or clay + silt has long been considered as a primary determinant of SOC stability and storage (Georgiou et al., 2025; Hassink, 1997; Matus, 2025; Oades, 1988; Parton et al., 1987; Six et al., 2002; Wiesmeier et al., 2019). However, studies across a range of soil types suggest that geochemical

* Corresponding authors.
E-mail addresses: morimaru.kida@people.kobe-u.ac.jp (M. Kida), wagai.rota200@naro.go.jp (R. Wagai).
[1] Present address: Research Center for Global Agromedicine, Department of Agriculture and Animal Science, Obihiro University of Agriculture and Veterinary Medicine, Inada, Obihiro, Hokkaido 080-8555, Japan.

https://doi.org/10.1016/j.geoderma.2026.117740
Received 10 September 2025; Received in revised form 13 February 2026; Accepted 13 February 2026
Available online 20 February 2026

properties, particularly reactive aluminum (Al) and iron (Fe) contents, may be a better predictor of SOC variations than clay or clay + silt contents (Matus et al., 2006; Percival et al., 2000), and that the relative importance of the predictors may vary with soil pH, climate, and biome (von Fromm et al., 2024, 2021; Rasmussen et al., 2018).

Reactive metals, including pedogenic Al and Fe (oxyhydr)oxides, short–range-order (SRO) minerals, organically complexed metals, and exchangeable metals, are commonly estimated using chemical extraction approaches. Sodium dithionite with citrate mainly targets reactive Fe mineral phases and their substituted Al mineral phases (Fe_{dc} and Al_{dc}). Acid ammonium oxalate mainly extracts both SRO Al and Fe minerals and organically complexed metals (Al_{ox} and Fe_{ox}). Sodium pyrophosphate is used to extract organically complexed metals (Al_p and Fe_p) (Parfitt and Childs, 1988). SRO minerals are thus often approximated by the difference between oxalate- and pyrophosphate-extractable metals (i.e., $Al_{ox} - Al_p$) (Parfitt and Childs, 1988). Among these metal phases, oxalate-extractable Al and Fe frequently emerge as the strongest predictor of SOC in a wide range of soils (Rasmussen et al., 2018), highlighting the potential importance of SRO minerals and organically complexed metals in SOC stabilization. However, the contributions of the specific reactive metal phases to SOC storage at the global scale remain poorly understood due to (i) substantial variation in parent material mineralogy, soil age, as well as climate-rock-SOC interactions, and (ii) the limited availability of datasets that include pyrophosphate-extractable metals (von Fromm et al., 2021; Hall and Thompson, 2022; Rasmussen et al., 2018).

Improved understanding of the role of specific metal phases in SOC storage can be achieved by constraining the state factors that govern soil formation (Jenny, 1941). Among the five state factors, climate, parent material, and time are typically the most influential at regional to global scales (von Fromm et al., 2021; Rasmussen et al., 2018; Torn et al., 1997). Andisols, which develop from a relatively constrained class of glass-rich volcaniclastic materials and represent early stages of pedogenesis (commonly Holocene in age, often <15,000 yrs) (Shoji et al., 1993), provide a unique opportunity to isolate these influences. Among volcaniclastic parent materials, Andisols most commonly develop from pyroclastic deposits (tephra), which are typically felsic to intermediate in composition in continental arc settings where magma differentiation and crustal assimilation promote explosive volcanism (e.g., the circum-Pacific "Ring of Fire"). These deposits dominate Andisol parent materials globally because their fine grain size, high volcanic glass content, and regionally extensive ash blankets promote rapid and laterally uniform development of andic soil properties (Delmelle et al., 2015; Shoji et al., 1993). To a lesser extent, Andisols can also develop from non-pyroclastic, mafic parent materials such as basaltic lava and hyaloclastite, particularly in oceanic and plume-related settings such as Hawaii and Iceland (Arnalds, 2004; Sato et al., 1973). Across these settings, Andisol parent materials are generally characterized by high contents of volcanic glass (metastable phases) and fine-grained fragmentation, resulting in high reactive surface area, rapid weathering, and accelerated formation of metal-rich soil constituents. The relatively narrow temporal window over which many Andisols develop further constrains parent material influence by reducing the likelihood of polygenetic processes such as repeated erosion and redeposition. By focusing on Andisols globally, we can more effectively examine how secondary metal phases formed through weathering control SOC storage, as soil geochemical variations primarily reflect the influence of climate on the weathering of a relatively uniform parent material.

Variations in Andisol have been categorized based on dominant metal phase (allophanic/silandic vs. non-allophanic/aluandic) and development time (vitric vs. andic) based on taxonomic criteria of andic soils (Shoji et al., 1993; Soil Survey Staff, 2014; IUSS Working Group WRB, 2015). Development of allophanic and non-allophanic Andisols is typically explained as follows (Shoji et al., 1993). When organic matter supply is limited (e.g., relatively recent volcaniclastic material with limited vegetation), Al cations and silicic acid released from volcaniclastic materials (esp. from volcanic glass) polymerize to form SRO aluminosilicates such as allophane and imogolite (Parfitt, 2009; Watanabe et al., 2023). On the other hand, under conditions of low pH, sufficient organic matter and water flux (typically in cooler, wetter climates), released Al ions preferentially react with organic acids to form organo-metal complexes, thereby suppressing SRO mineral formation (Takahashi & Dahlgren, 2016). Regionally, aeolian dust inputs contribute to the formation of non-allophanic Andisol due to accelerated acidification as dust-derived 2:1 phyllosilicate clays with permanent negative charges retain exchangeable protons and Al under low pH, humid conditions (Eguchi et al., 2012; Inoue and Naruse, 2009; Shoji, 1985). More recently, the formation of non-allophanic surface horizon over allophanic horizon through dissolution of SRO aluminosilicates under acidic condition (pH < 5) with abundant organic matter has been suggested (Alam et al., 2025; Zieger et al., 2026). From a pedogenic time perspective, fresh volcaniclastic materials (Entisol) progress to glass-rich "vitric" Andisols and later to allophane-rich "andic" Andisols abundant in SRO minerals and/or organo-Al complexes and, ultimately, to more strongly weathered soils including Spodosols, Alfisols, Mollisols, Ultisols, and Oxisols depending on climate, time, and parent material composition (Ugolini and Dahlgren, 2002). Chronosequence studies in volcanic regions such as Hawaii and the west coast of North America, Sierra Nevada (Mexico), and Sicily (Italy) provide strong evidence for these mineralogical transitions and associated changes in mineral protection of SOC (Egli et al., 2008; Lilienfein et al., 2003; Mikutta et al., 2009; Peña-Ramírez et al., 2009; Torn et al., 1997).

We compiled a global Andisol database to expand an existing dataset (Shoji et al., 1996) by incorporating samples from a broader range of geographic and pedogenic environments (Fig. 1), with the goal of identifying the key factors driving variation in SOC content across a wide range of pedogenic (largely climate-driven) conditions. As parent material and time are relatively constrained, our working hypothesis in this study was that climate, and the associated variation in soil pH, exerts a dominant control on metal phases and their relationships with SOC. Specifically, we tested the following hypotheses.

(*H1*) Secondary Al phases—particularly organically complexed Al—better predict SOC variations than secondary Fe phases because Al exhibits stronger polarizing power and a higher ability to form stable inner-sphere complexes with organic ligands, resulting in persistent organo-Al associations (Boudot et al., 1989; Scheel et al., 2007; Sparks, 2003; Wada and Higashi, 1976). This hypothesis was tested by comparing the relative importance of Al- versus Fe-related extractable metal contents across the full global dataset.

(*H2*) SOC–metal relationships shift with pedogenesis from vitric to andic stages. By classifying the dataset into four groups based on combinations of soil development stage (vitric versus andic) and dominant reactive Al phases (allophanic versus non-allophanic), we examined whether important predictors of SOC content changed over Andisol development.

(*H3*) Climatic factors and soil pH systematically modulate SOC–metal relationships. Pedogenesis is fundamentally driven by the consumption of acidity during chemical weathering of parent materials, with acidification progressing from base-cation buffering towards Al-dominated buffering systems, where the soil components controlling pH shift in a systematic and predictable manner (Chadwick and Chorover, 2001). We tested this hypothesis by stratifying the dataset into sub-datasets spanning major climatic zones and soil pH classes, allowing examination of whether important predictors of SOC content vary systematically along climatic and acid–base gradients.

Non-linear statistical models were used to test above hypotheses while accounting for the depth in soil profile for each Andisol samples. This approach allowed us to overcome key limitations identified in previous studies of SOC-soil property relationships in Andisols (Lyu et al., 2021; Matus et al., 2008, 2006; Percival et al., 2000; Takahashi et al., 2012), including restricted geographical coverage, the exclusion of climate and soil depth as explanatory variables, and the failure to

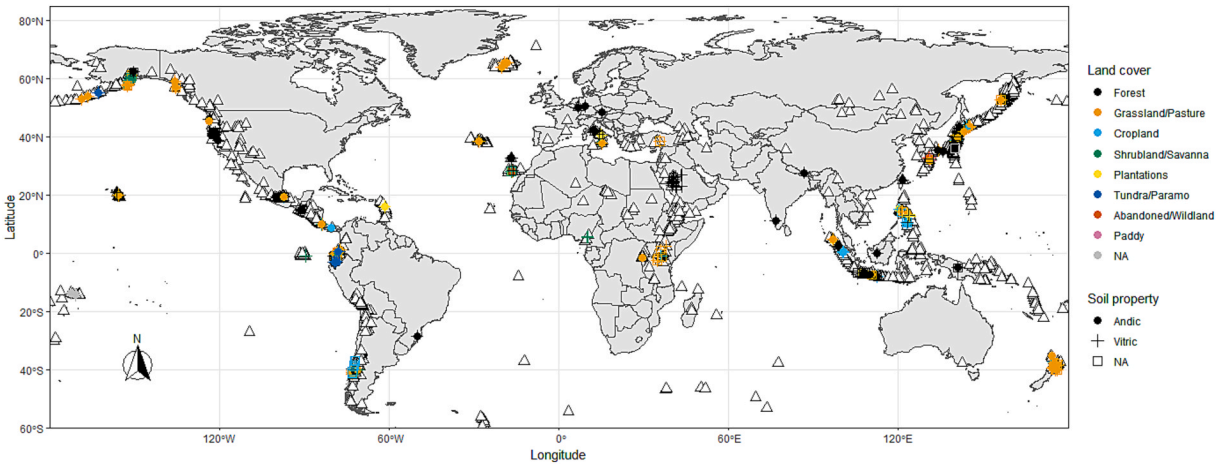

Fig. 1. Map showing the distribution of the pedons in the global Andisol dataset, with the soil property being assigned to each horizon. Volcanoes are also mapped with the white triangles (data from Sigl et al. 2015, where submarine volcanoes were excluded). Map lines delineate study areas and do not necessarily depict accepted national boundaries. NA = not assigned. The map was recreated using data from Kida et al. (2025).

account for non-linear relationships between geochemical and climatic factors with SOC. Substantial work has been done on Andisol genesis and properties (Dahlgren et al., 2004; Shoji et al., 1993) including the role of reactive metal phases on SOC storage and stabilization (Matus et al., 2014; Takahashi and Dahlgren, 2016; Wada, 1985).

We examined how pedogenic factors (esp. climate-driven pH variation) and processes regulate reactive Al and Fe phases and their associations with SOC using the expanded Andisol dataset including over 2850 soil samples collected across more than 30 countries, spanning a broad range of climate and soil pH conditions, and explored their mechanistic linkage to broader soil chemical and pedogenic processes. Throughout this study, reactive Al phases are defined in a pedogenic–geochemical sense to include both mineral forms, such as SRO Al minerals quantified as $Al_{ox} - Al_p$, and non-crystalline phases such as organo-Al complexes quantified as Al_p, which coexist with dissolved and exchangeable Al pools.

2. Materials and methods

We created an extended Andisol database by expanding from the Tohoku University World Andosol Database (TUWAD) (Shoji et al., 1996) using the approach shown below. The updated SOC storage estimates of global Andisols using this database was reported elsewhere (Kida et al., 2025).

2.1. Literature search

Nearly half the data analyzed (260 pedons, 1453 horizons) were obtained from TUWAD (Shoji et al., 1996). All data in the TUWAD were manually checked by referring to the original publications, and any typographical errors, missing data in calculations, or incorrect placements of zeros where they should have been blanks, were corrected. Additional data were collected through a literature search in English on Web of Science, with the following search terms: “Andosol organic matter”, “Andisol organic matter”, “Andosol organic carbon”, “Andisol organic carbon”, “volcanic ash soil organic matter”, and “volcanic ash soil organic carbon”. Each literature search yielded a few hundred papers, which were screened based on their title, abstract, and full text. Our literature search was conducted for papers published from 1994 onwards (i.e. post-compilation of TUWAD) and was completed in November 2021. We excluded O and R horizons from TUWAD and the newly compiled dataset if they were reported, as we focused on mineral soil horizons. In total, we gathered 2854 horizons from 574 pedons across 34 countries including the data from TUWAD (Fig. 1). Subsequently, SOC data estimated by the Walkley-Black wet oxidation method (n = 1193) were converted to combustion-C equivalent by multiplying a generally accepted correction factor of 1.3 (Walkley and Black, 1934). When some correction factors were already applied in the literature, we back-transformed reported values to original values and then multiplied them by a factor of 1.3. While a universal correction factor to estimate SOC content for all soils does not exist (Lettens et al., 2007), this correction is necessary to minimize biases associated with wet oxidation method among various studies. Samples with SOC content of ≥25% (by weight) were excluded, as such soil is classified as organic (Soil Survey Staff, 2014) and out of the scope of this study. Data on soil texture were removed if the dispersion treatment of clay particles was deemed incomplete due to the use of sodium hexametaphosphate (or *calgon*) as a dispersant which is not recommended for Andisols (Nanzyo et al., 1993; Ping et al., 1988). The maximum clay dispersion in Andisols is known to be achieved by pH adjustment and ultrasonication (Asano and Wagai, 2014; Nanzyo et al., 1993; Silva et al., 2015).

2.2. Screening

We further screened the dataset to include only those horizons that meet taxonomic criteria for andic or vitric soil properties, defined as (IUSS Working Group WRB, 2015):

Andic properties require:

1. *An $Al_{ox} + 1/2Fe_{ox}$ value of ≥2%; and*
2. *A bulk density of ≤0.9 kg dm^{-3}; and*
3. *A phosphate retention of ≥ 85%*

Vitric properties require:

1. *≥5% (by grain count) volcanic glass, glassy aggregates and other glass-coated primary minerals, in the fraction ≥0.02 and ≤2 mm; and*
2. *An $Al_{ox} + 1/2Fe_{ox}$ value of ≥ 0.4%; and*
3. *A phosphate retention of ≥ 25%*

where Al_{ox} and Fe_{ox} represent Al and Fe extracted by a pH 3 acid ammonium oxalate solution. When the bulk density of a given horizon was not reported, it was estimated by calculating the average bulk density of other horizons in the same pedon. If no bulk density was available for any horizons of the pedon, we estimated the bulk density from an empirical relationship between SOC content (in %) and bulk density (for samples with %SOC < 25; bulk density = $0.9481 \times e^{-0.054 \times SOC}$, $R^2 = 0.41$, root mean squared error = 0.26, n = 1773)

established using all available data in the dataset. When the data for only one of the three criteria was missing, such a horizon was retained if the other two criteria were met. This less-stringent modification was necessary due to a large number of missing data, especially volcanic glass content; otherwise, a large part of vitric horizons would have been screened out. If a horizon met both the andic and vitric properties, such horizon was classified as andic. In our dataset, 1290 horizons in 340 pedons from 29 countries met the andic criteria, while 977 horizons in 345 pedons from 32 countries met only the vitric criteria. There were 146 pedons that had only andic horizons, 151 pedons that had only vitric horizons, and 194 pedons that had both andic and vitric horizons.

2.3. Geochemical, climatic, and vegetation variables

We collected data on soil geochemical, climatic, and vegetation variables for statistical analyses to evaluate the key factors influencing the spatial variation in SOC content in Andisols. Geochemical properties considered in this study included soil pH in H_2O measured with a soil-to-water ratio of 1:2.5 and reactive metal phases that included 0.2 M oxalate-extractable aluminum (Al_{ox}) and iron (Fe_{ox}), 0.1 M pyrophosphate-extractable aluminum (Al_p) and iron (Fe_p), and their differences (Al_{ox}-Al_p and Fe_{ox}-Fe_p). Pyrophosphate-extractable Al and Fe represent the amount of organically complexed metals with minimal dissolution of SRO Al/Fe minerals (such as allophane, imogolite, and ferrihydrite). Acid oxalate extracts both organically complexed metals and poorly crystalline Al and Fe oxide phases including SRO minerals. The differences in extractable metals between the two methods (i.e., Al_{ox}-Al_p and Fe_{ox}-Fe_p) approximately represent SRO Al (allophane and imogolite) and Fe (ferrihydrite) minerals, respectively (Parfitt and Childs, 1988). However, as these extractions are not highly selective, it should be noted that the metals extractable by sodium pyrophosphate and acid oxalate reagents only roughly correspond to specific metal phases (Rennert, 2018). Exchangeable calcium (Ca_{ex}) as determined by ammonium acetate extraction at pH 7.0 or clay content, or both, was included in separate statistical analyses due to the limited availability of the data for these variables. Climatic variables included mean annual temperature (MAT) and mean annual precipitation minus potential evapotranspiration (MAP-PET), which were estimated by TerraClimate (data between 1958 and 2019, ~5 km resolution) (Abatzoglou et al., 2018). Net primary production (NPP) data was estimated by MODIS/Terra Net Primary Production (MOD17A3HGF v006, data between 2000 and 2021, 500 m resolution) (Running and Zhao, 2021). Land use information was extracted from each paper, but when missing, it was estimated by Copernicus Global Land Cover Layers (CGLS-LC100 Collection 3, data between 2015 and 2019, 100 m resolution) (Buchhorn et al., 2020), and subsequently summarized into eight categories (See Fig. 1).

2.4. Statistical analysis

All statistical analyses were conducted in *R* (version 4.3.0; https://www.r-project.org/). We first examined possible systematic differences in geochemical and climatic characteristics among the four Andisol groups based on the soil development stage (vitric versus andic) and dominant reactive Al phases (allophanic versus non-allophanic). Vitric and andic properties were determined according to the WRB classification system, while allophanic and non-allophanic properties were defined by the Al_p/Al_{ox} ratio of below and above 0.5, respectively (Shoji et al., 1996). Difference in these variables between the groups was tested by the Wilcoxon rank sum and considered significant at $p < 0.01$. We then tested whether general soil-forming factors and SOC contents between Al-rich (or proto-imogolite) allophane and Si-rich allophane soils differ (Parfitt, 1990). Al-rich allophane typically has an Al/Si ratio of 2, whereas Si-rich allophane has a ratio of 1 (Parfitt, 1990; Watanabe et al., 2023). We also examined the variability in the SOC-to-Al_p molar ratio (SOC/Al_p) under different temperature and moisture regimes and pH and NPP ranges to test if the nature of organo-Al complexes was dependent on these variables. Results and discussions related to these analyses are provided in Supporting Information for parsimony (Supplementary Discussion S1, S2, Figs. S1, S2).

To test *H1*, we used a generalized additive mixed model (GAMM) implemented in the "*mgcv*" package (Wood, 2022) to identify the set of variables that best explained variation in SOC content while accounting for possible nonlinear relationships between predictors and SOC (Yu et al., 2021). Details are provided in Supplementary Methods. Briefly, the horizon midpoint depth, soil geochemical properties, climate variables, and net primary production (NPP) were used as standardized (Z-scored) fixed effects to account for differences in scale. We used thin plate regression splines for each term in the model (Wood, 2003). Because of the positive continuous nature and right-skewed distributions of SOC content, we fitted a GAMM with a Gamma family using a log-link function. Importantly, this approach differs from fitting a GAMM with a Gaussian family on log-transformed SOC (see Supplementary Methods). The model performance was quantified using the deviance explained, which is a generalization of R^2 and can be interpreted similarly (P84, (Wood, 2006). We optimized the fixed effects and the random effect structure so that the model fit by maximum likelihood had the lowest Akaike's information criterion (AIC). The final model ($n = 1383$, no missing data) included depth, Al_p, Al_{ox}-Al_p, Fe_p, pH, MAT, and NPP as the fixed effects and random slopes of the depth effect based on the pedon as well as random intercepts based on the study. The significance of model terms was estimated using approximate *F*-values. We also used a GAMM to identify the variables that best explained the variation in Al_p content, using depth, pH, MAP-PET, MAT, and NPP as the predictors ($n = 1715$, no missing data). The predicted relationships between SOC and predictors were presented in the original scale of predictors by reverse Z-scoring, using R packages "*gratia*" (Simpson, 2023) and "*ggplot2*" (Wickham, 2016).

To gain mechanistic understanding of the results of the GAMM analysis, we tested whether molar ratios of Fe_p/Al_p and (Fe_{ox}-Fe_p)/(Al_{ox}-Al_p) vary with soil pH or MAP-PET. These ratios represent the Fe/Al ratios of the organically complexed phase and SRO minerals, respectively. As we were interested in the overall trend in the Fe/Al ratios along these variables, generalized additive models (GAMs) were used with soil pH or MAP-PET as the fixed effect. We used thin plate regression splines for each term in the model, with a Gaussian family (Wood, 2003). The content of allophane in soil samples was also estimated to estimate the maximum contribution of allophane to SOC content via organic matter sorption, using the following equations (Mizota and Reeuwijk, 1989).

$$\%\text{Allophane} = \%Si_{ox} \times 100/y \quad (1)$$

where

$$y = 23.4 - 5.1 \times \left(\%Al_{ox} - \%A_p\right)/\%Si_{ox} \quad (2)$$

To test *H2*, we fitted GAMMs to subsets of samples grouped according to the combinations of the soil development stage and dominant reactive Al phases, to identify the factors that influenced the SOC content within each Andisols type. To test *H3*, we applied GAMMs to subsets of samples sorted by pH, MAT, or MAP-PET classes to examine whether influential factors (pH, Al_p, Al_{ox}-Al_p, or Ca_{ex}) on SOC content vary with these variables. Details of these analyses and the number of samples in each model are provided in Supplementary Methods and in Table S1. These GAMM analyses of sub datasets allowed us to quantitatively assess relative contributions of specific metal phases along climatic and acid–base gradients as well as with pedogenic development, which was not possible with the full global model. In all models, we quantified the contribution of each covariate using ΔAIC, defined as the AIC increase between the reduced and full models with each smooth term removed. ΔAIC measures the loss of predictive information attributable to each covariate, accounting for both goodness-of-fit and the penalty on

smoothness (Wood, 2006). To facilitate comparison across covariates and different models, ΔAIC values were normalized by the sum of all ΔAIC values within each model, yielding a relative importance metric (% of total ΔAIC).

3. Results

3.1. General characteristics of Andisols

Soil pH of the samples compiled ranged between 3.1 and 9.3 and declined with the increase in annual water balance (i.e., MAP-PET, Fig. 2). The pH histogram showed that samples were largely clustered at pH 4.5–6.5 with the peak at around 5.5 particularly for allophanic Andisols under wetter climate (Fig. 2).

The observed variations in geochemical characteristics among the compiled Andisol samples were partly explained by distinguishing the four Andisol groups based on the combinations of soil development stage (andic versus vitric) and dominant reactive Al phases (allophanic versus non-allophanic) (Fig. 3). All geochemical variables (such as SOC, TN, Fe, Al, and other cations) showed variations spanning two to three orders of magnitude, whereas climate and vegetation variables (MAT, MAP-PET, and NPP) differed by one to two orders of magnitude across the data points (Figs. S3, S4). The environmental conditions favoring the formation of allophanic and non-allophanic Andisol groups were distinct, with the latter characterized by higher SOC content and lower pH (Fig. 3a, d). When comparing allophanic versus non-allophanic soils, non-allophanic soils had higher SOC (median 7.6%, n = 630 versus median 2.9%, n = 1299, $p < 0.01$, Fig. 3a, Fig. S3), lower pH (median 5.0, n = 624 versus median 5.8, n = 1175, $p < 0.01$, Fig. 3d, Fig. S3), and higher Al_p and Fe_p contents (Al_p: median 1.2%, n = 630 versus median 0.42%, n = 1299, $p < 0.01$, Fig. S3; Fe_p: median 0.94%, n = 564 versus median 0.12%, n = 931, $p < 0.01$, Fig. S3) than allophanic soils. The higher median SOC content of non-allophanic soils was due primarily to a more even distribution of SOC, rather than to a greater number of horizons with high SOC (Fig. S6). In addition to SOC content, C:N ratio in non-allophanic soils (median 18.2, n = 272) was higher than that in allophanic soils (median 14.2, n = 514, $p < 0.01$, Fig. 3b, Fig. S3), implying slower organic matter decomposition rate and/or larger abundance of high C:N compounds such as phenolic and pyrogenic C in non-allophanic soils. When comparing vitric versus andic soils, andic soils had higher SOC contents (median 5.3%, n = 1097) than vitric soils (median 1.8%, n = 832, $p < 0.01$) with no clear difference in C/N ratios (~ 15) (Fig. 3b, Fig. S4). Soil bulk density varied among the four groups showing inverse patterns to SOC content (Fig. 3c). The content of SRO Al and Fe minerals, approximated by $Al_{ox} + 1/2\ Fe_{ox}$, was higher in andic than vitric soils and in allophanic than non-allophanic soils, as expected (Fig. 3e). Both Al_p/Al_{ox} and Fe_p/Al_p ratios were significantly higher in non-allophanic soils (Fig. 3f, g). Climatic variables had no clear differences among the different soil groups (Fig. 3h, i).

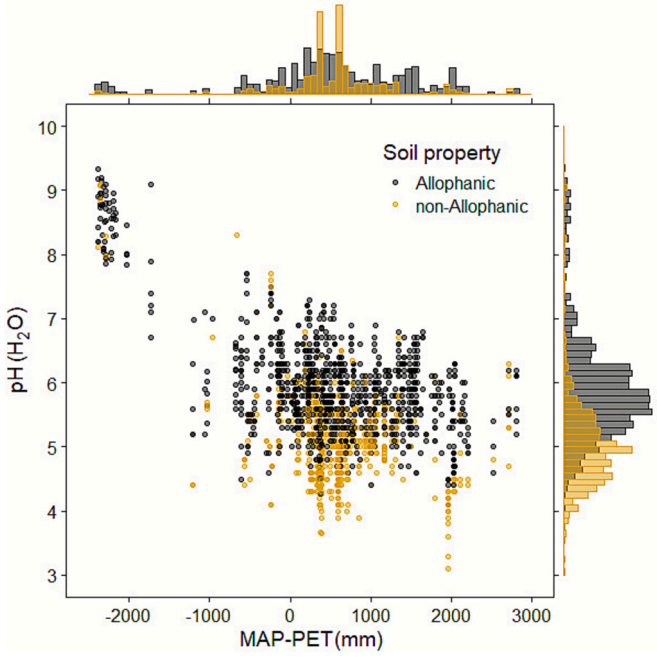

Fig. 2. Soil pH versus annual water balance. Black and orange dots represent raw data for allophanic (silandic) and non-allophanic (aluandic) soils, respectively, while side panels show histograms of pH and mean annual temperature (MAP) minus potential evapotranspiration (PET) for each type of soils.

3.2. Determinants of SOC variations: geochemical factors and metal chemistry

3.2.1. Limited effect of clay content control

The relative importance of the examined variables shifted when the GAMM models included either "clay content", "Ca_{ex}", or both in addition to the other variables selected in the main model (Table S2, Figs. S7-S9). When clay content alone was included in GAMMs, it was one of the poorer predictors for SOC (Table S2, Fig. S8). Clay content had a positive but weak predictive influence on SOC only for soils with low clay content (approximately < 20%), contrary to the strong and exponential influence of Al_p in the full observed range (Fig. S8). When both clay and Ca_{ex} contents were considered, clay content was not a significant predictor of SOC (Table S2, Fig. S9). It should be noted that the measurement of clay content in Andisols is prone to errors due to incomplete dispersion of physically stable aggregates (Asano and Wagai, 2014). However, this error should not significantly affect the present results because we excluded the clay content data in our analysis if the dispersion of clays was deemed incomplete due to the use of sodium hexametaphosphate as a dispersant (Nanzyo et al., 1993; Ping et al., 1988).

3.2.2. Greater significance of Al over Fe

Our GAMM analysis for the global dataset indicated that organically complexed Al (Al_p) was by far the strongest predictor of SOC content, followed by SRO Al minerals (Al_{ox}-Al_p), after accounting for depth effect (Table 1, Fig. 4). Soil pH and Fe_p were also significant predictors of SOC although their relationships with SOC varied depending on their ranges (Fig. 4). In contrast with Al_p, the importance of Fe_p was much lower, showing only for the soils with approximately < 1% Fe_p and low SOC content. Furthermore, SRO Fe minerals (Fe_{ox}-Fe_p) were not a significant predictor of SOC. NPP was predicted to have a small positive effect on SOC, indicating weak control by vegetation carbon inputs, but this effect may be underestimated due to uncertainty in NPP estimates.. Among the climatic variables used, only MAT had a significant impact on SOC, though the relationship was weak and fluctuating (Fig. 4). These results indicate that variation in SOC in Andisols is primarily associated with reactive Al phases, with Fe phases and climate variables exerting secondary influences.

Organo-Al complexes (Al_p) were more abundant than organo-Fe complexes (Fe_p) for 96% of the samples (median Fe_p/Al_p molar ratio of 0.27). The increase in Fe_p occurred with decreasing soil pH especially < 4.5 (Fig. 5a). SRO Al minerals were also more abundant than SRO Fe minerals in 87% of the samples (Fig. 5b). The median Fe/Al molar ratio for SRO minerals was 0.26, closely matching that of organo-metal complexes (Fig. 5a), suggesting that the partitioning of these two metals into both organo-metal complexation and SRO minerals may be governed by a common mechanism. The observed non-linear Fe_p/Al_p with pH (Fig. 5a) likely reflects differences in hydrolysis behavior between Fe and Al, as Fe undergoes hydrolysis at lower pH (pKa) than Al (Chadwick and Chorover, 2001). The abundance of SRO Al minerals peaked at pH 5.5–6.2 (Fig. S10), consistent with the optimal pH

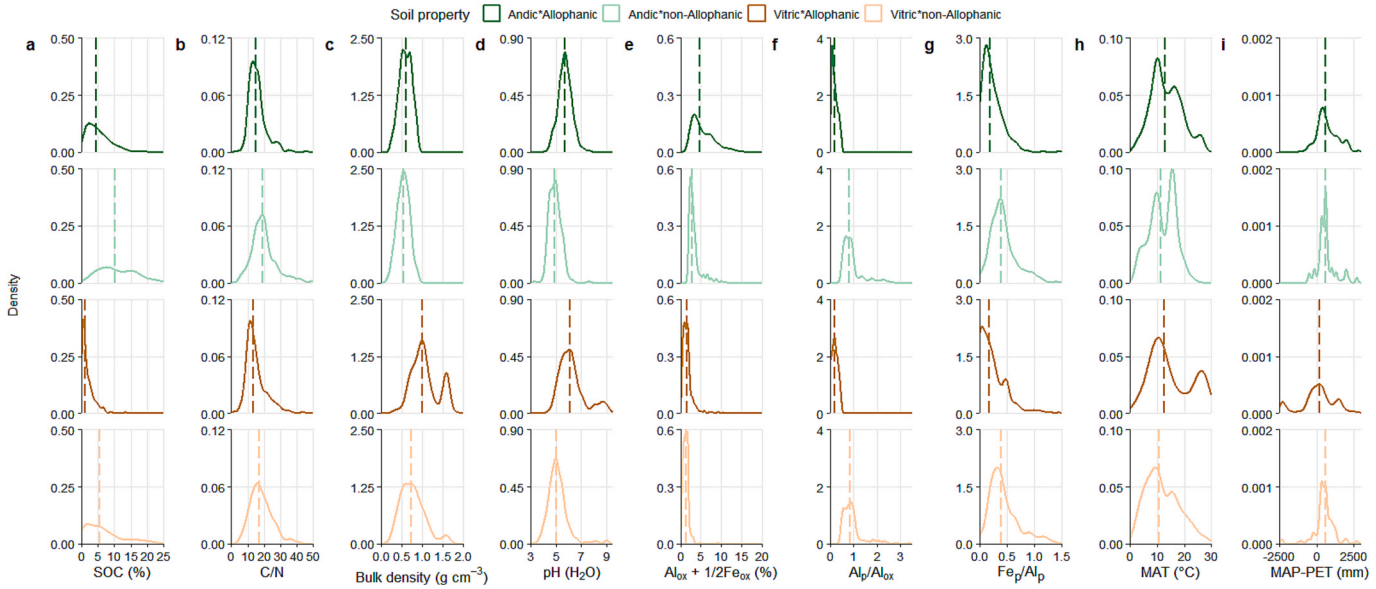

Fig. 3. Density distribution of geochemical and climatic characteristics of Andisols according to the combinations of the soil development stage and dominant reactive Al phases. Dashed vertical lines represent the median value for each group.

Table 1
Fixed-effect variables from the generalized additive mixed model of SOC content (Deviance explained = 88.1%). Only significant predictors ($p < 0.01$) are provided and ordered in a descending order of their relative importance determined by ΔAIC[†].

Predictors	EDF	*F*-value	ΔAIC	Relative importance (%)
Al_p	6.642	47.407***	327	40.3
Depth	6.833	90.169***	240	29.5
Al_{ox}-Al_p	2.698	28.839***	82.7	10.2
pH(H_2O)	5.426	9.766***	75.9	9.34
Fe_p	7.114	7.881***	47.3	5.82
NPP	1	18.228***	2.78	2.78
MAT	5.769	3.854***	2.10	2.10

EDF = Effective degree of freedom.
*** p-value < 0.001.
† Exchangeable Ca and clay content were not considered due to the liSmited sample numbers that included these geochemical variables. See Table S2 for models with these variables included.

condition of 5–7 for the secondary formation of allophane and imogolite from volcaniclastic parent materials (Dahlgren et al., 2004). While SRO Fe minerals are generally more susceptible to reductive dissolution than SRO Al minerals, we detected no significant decrease in the Fe phase relative to the Al phase under wetter conditions (Fig. 5d). Interestingly, Al_p/Al_{ox} and Fe_p/Fe_{ox} ratios showed very similar patterns along soil pH and MAP-PET (Fig. S11). These ratios increased sharply at pH < ~6 but showed no clear trend with MAP-PET (Fig. S11).

3.3. pH dependency of metal phases and their predictive power

Further GAMMs analysis was conducted to examine the extent to which environmental factors affect the relative importance of specific metal phases that account for SOC variation (Fig. 6). The importance of Al_p was almost always the highest but declined sharply at median pH ≥ 6.3 (Fig. 6a). The importance of Al_p increased linearly with increasing annual water balance (Fig. 6c), while no such clear trend was found with temperature (Fig. 6b). SRO Al minerals (Al_{ox}-Al_p) were not significant (at 0.01 level) at extreme pH ranges (median pH ≤ 4.8 or median pH ≥ 6.8) and their importance was always lower than that of Al_p across the pH gradient (Fig. 6a). Importantly, Ca_{ex} became significant at the median pH ≥ 5.7 and its importance increased considerably at the median pH ≥ 6.3. At above this pH, Ca_{ex} exceeded the importance of Al_p (Fig. 6a), which corresponded to the sharp decline in Al_p content from pH 4.5–5.5 towards pH 7 (Fig. S10a). Consistent with these GAMM results, Al_p increased with decreasing soil pH especially < 6, whereas Al_{ox}-Al_p showed a maximum at approximately pH 5.5 (median 1.2%, interquartile range 0.3%–3.0%, n = 1584) and decreased sharply above and below this pH (Fig. S10a, c). The contents of both Al_p and Al_{ox}-Al_p were very low at alkaline pH > 7. The variation in Al_p content was strongly influenced by soil pH with the maximum Al_p level at soil pH 4.5–5 (Fig. 7a) and, to some extent, by annual water balance (Fig. 7d).

3.4. Pedogenic stage and SOC–metal relationships

To clarify how pedogenic stage shapes SOC–metal interactions, we fitted GAMMs separately for the four Andisol groups. Across these groups, even in the two allophanic groups, SRO Al mineral content was a much less important SOC predictor than organically complexed Al (Fig. 8). In the less developed (vitric) Andisols, SRO Al mineral was not a significant variable (Table S3). From a pedogenic perspective, it is noteworthy that Al_p exerted a stronger influence on SOC in more developed andic soils than the younger vitric soils when comparing the corresponding allophanic or non-allophanic groups (Fig. 8).

4. Discussions

Our working hypothesis was that climate, and the associated variation in soil pH, exerts a dominant control on metal phases and their relationships with SOC. Accordingly, we first discuss climate-driven pedogenic processes that affected the reactive metal phases and their pool sizes, followed by an evaluation on how specific metal phases likely influence SOC storage and its implications for SOC persistence.

4.1. pH driven controls on reactive Al phases

Analysis of the extended Andisol database revealed strong coupling among climate, soil pH, and soil chemical and mineralogical responses, highlighting soil pH as a key integrator of climatic and pedogenic controls on reactive Al phases. The observed peak in soil pH at ~5.5 (Fig. 2) is consistent with the acidic-side threshold identified in a global subsoil dataset (Slessarev et al., 2016) and suggests that most Andisol samples are near chemical equilibrium with respect to dominant acid-base

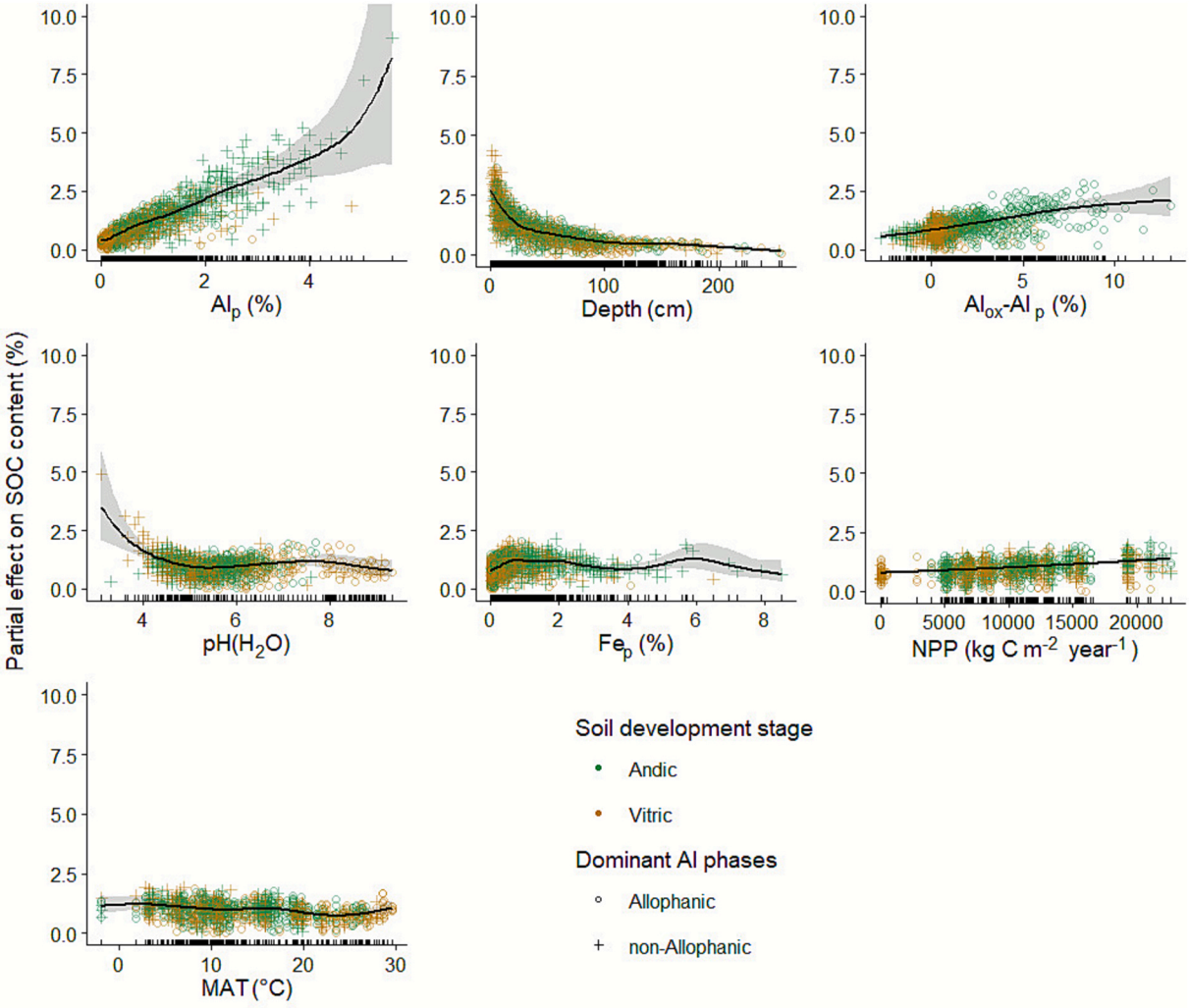

Fig. 4. Generalized additive mixed models (GAMMs) showing the partial effects of geochemical and climatic predictors on soil organic carbon (SOC) content. The random effects considered are a random slope of the depth effect based on the soil pedon and random intercepts based on the study (Deviance explained = 88.1%). The tick marks on the x-axis show the distribution of observed values (rug plot). The solid lines represent the estimated smooth function, while shading represents the 95% confidence intervals. The superimposed points, colored and marked depending on dominant Al phases and soil development stage, are partial residuals which show the relationship between a given independent variable and the response variable after accounting for influences from the other covariables. Plots are ordered in a descending order of relative importance (Table 1).

reactions. Pedogenically, protons (acidity) generated by atmospheric and respiratory CO_2 as well as organic acids (particularly under greater water input) are consumed through the weathering of volcaniclastic parent materials and the reactions involving exchangeable complexes (Ugolini and Dahlgren, 2002). Under acidic conditions, soil pH is therefore largely regulated by Al hydrolysis reactions in soil solution, with dissolved Al activities buffered by equilibrium with reactive Al phases (e.g., Al hydroxides and SRO Al minerals) and associated dissolved and exchangeable Al species (Chadwick and Chorover, 2001).

Across the pH gradient, two major reactive Al phases, organically complexed Al (Al_p) and SRO Al minerals (Al_{ox}-Al_p), co-occurred in most Andisol samples, but their relative abundance varied systematically with pH (Fig. S10a, c, S11a,c). Under alkaline conditions (pH > ~7), typically associated with drier climates (Fig. 2) and carbonate (mainly $CaCO_3$) buffering, high base saturation and low dissolved Al availability suppress the formation of both organo-Al complexes and SRO Al minerals. Under such conditions, elevated dissolved Si from volcanic glass dissolution can favor halloysite dominance in the colloidal fraction (Wada et al., 1987; Wada and Kakuto, 1985). As soil acidifies under wetter climates, carbonate buffering diminishes and, at pH around 5.5, dominant exchangeable cations shift from non-hydrolyzing base cations to Al species. Near pH ~5.5 where Al hydroxide solubility is minimized and Al hydrolysis is most active, SRO Al minerals reached maximum abundance (Fig. S10c), consistent with previous reports (Dahlgren et al., 2004).

Further acidification below pH ca 5.5 is characterized by increasing concentrations of monomeric Al in soil solution and exchange sites, together with elevated organic acid inputs reflecting less complete organic matter decomposition and enhanced organo-metal coprecipitation under acidic conditions (Chadwick and Chorover, 2001; Scheel et al., 2008; Takahashi and Dahlgren, 2016; Tonneijck et al., 2010). With further acidification below pH ~5.5, increasing Al solubility and hydrolysis elevate dissolved Al concentrations, promoting strong complexation with organic ligands even as ligand protonation increases, because Al^{3+} can bind effectively to partially deprotonated functional groups. To a lesser extent, reactive Fe phases exhibit similar behavior, as reflected by comparable pH-dependent patterns of Al_p/Al_{ox} and Fe_p/Fe_{ox} ratios (Fig. S11).

The high affinity of Al for organic ligands and the relative stability of the resulting complexes, combined with weak competition from silicic acid at anion exchange sites, further promote organo-Al complex formation and Si leaching (Jansen et al., 2003; Klotzbücher et al., 2020;

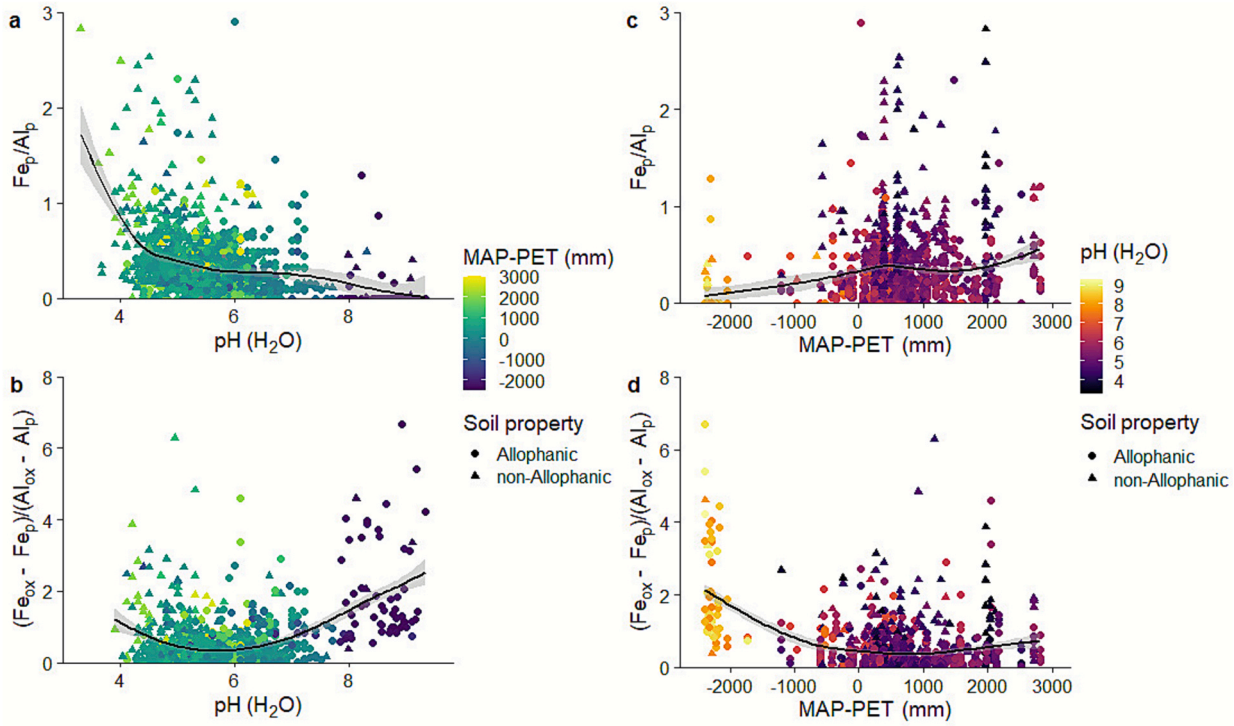

Fig. 5. Fe$_p$/Al$_p$ and (Fe$_{ox}$-Fe$_p$)/(Al$_{ox}$-Al$_p$) molar ratios versus soil pH (a, b) and MAP-PET (c, d). The Fe$_p$/Al$_p$ and (Fe$_{ox}$-Fe$_p$)/(Al$_{ox}$-Al$_p$) ratios represent the Fe/Al ratios of the organically complexed phase and poorly crystalline oxide phase, respectively. The regression in each panel represents a significant trend ($P < 0.0001$) along the x-axis by a generalized additive model (GAM).

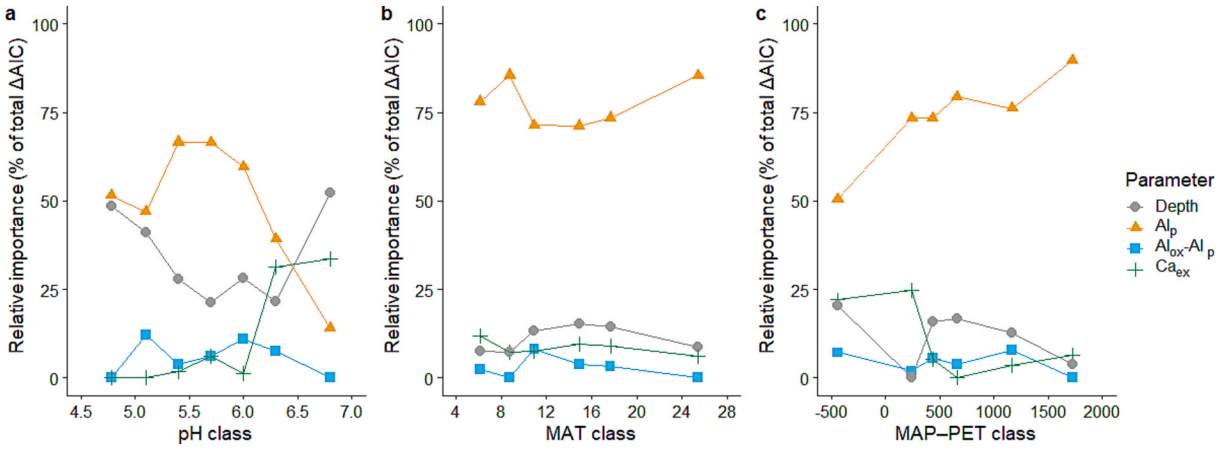

Fig. 6. Variable importance of covariates in generalized additive mixed models (GAMMs) for SOC content across pH (a), MAT (b), and MAP-PET (c) classes. The random effects are the same as in the main model (see Fig. 4), while only variables shown in the legend are considered. The x-axis shows the median values of samples in each class.

Nierop et al., 2002; Scheel et al., 2007). Consequently, rapid weathering of volcanic glass in surface horizons under vegetation typically leads to the formation of reactive Al phases including organo-Al complexes and SRO aluminosilicate, together with amorphous opaline Si from the leached Si (Shoji et al., 1993).

Consistent with this framework, Al$_p$ increased sharply with soil acidification particularly below pH ~6 (Fig. S10a) and reached a maximum around pH 5 (Fig. 7a), closely matching key pK values for Al hydrolysis in solution. Al$_p$ content also increased under wetter sites (Fig. 7d), indicating that climate-driven water balance (i.e., net water percolation through soil) indirectly regulates reactive Al speciation by controlling soil pH and Al solubility.

4.2. pH dependent predictors of SOC storage: Ca and reactive Al and Fe phases

Among candidate predictors of SOC variations, we evaluate the relative importance of texture (%clay) and exchangeable Ca, extractable Al versus Fe phases, and organo-Al complexes versus SRO Al minerals.

4.2.1. Minor role of clay content and limited role of calcium

Limited explanatory power of clay content for SOC variation in Andisols found in this study confirms the previous observations from Andisols and other soil types (Arai et al., 2025; Ashida et al., 2021; Fukumasu et al., 2021; Matus et al., 2014, 2006; McNally et al., 2017; Rasmussen et al., 2018; Salonen et al., 2024). In fact, decomposition rate

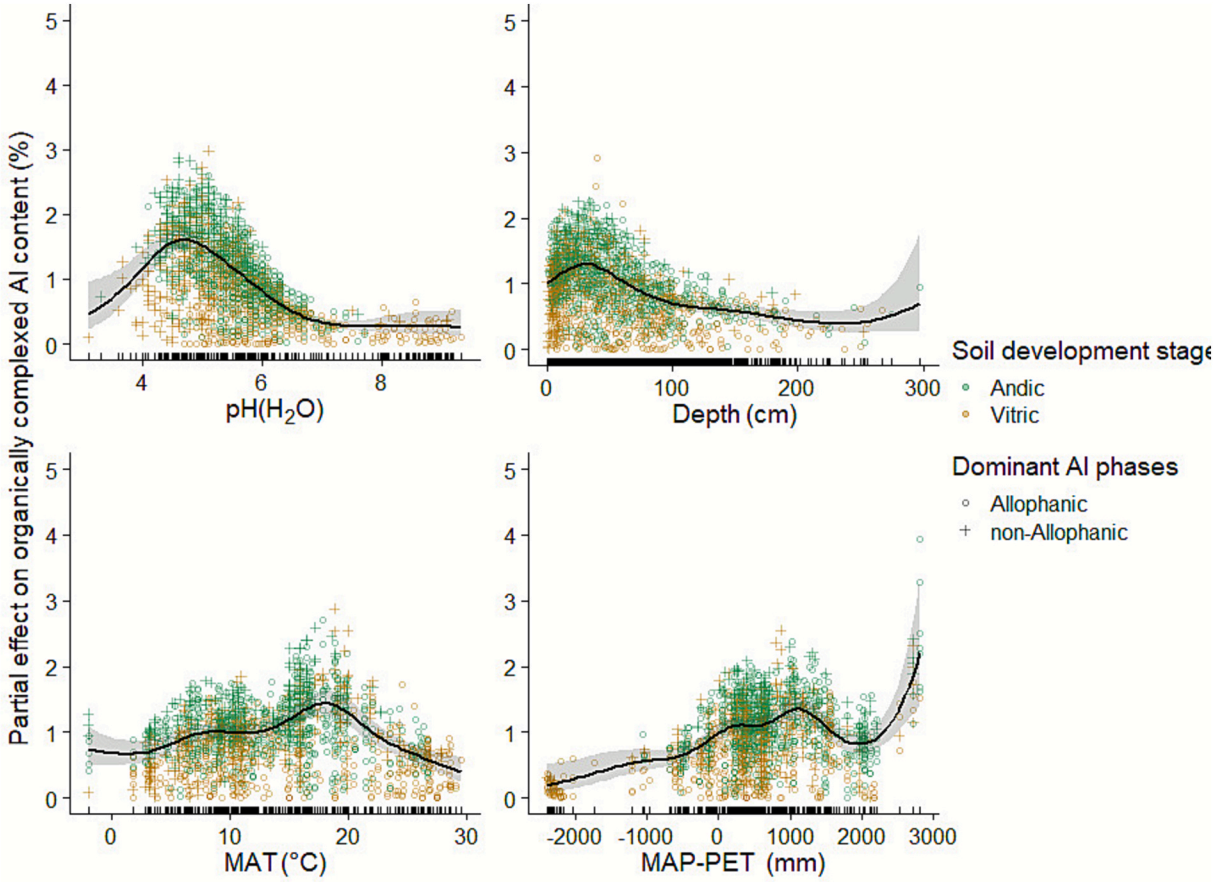

Fig. 7. Generalized additive mixed models (GAMMs) showing the partial effects of geochemical and climatic predictors on organically complexed aluminum (Al_p) content estimated by pyrophosphate extraction. The random effects are the same as in the main model (see Fig. 4) (Deviance explained = 77.6%). F-values for pH, depth, MAT, and MAP-PET are 52.638, 23.921, 9.171, and 9.161, respectively. We refer the reader to Fig. 4 for the interpretation of this figure.

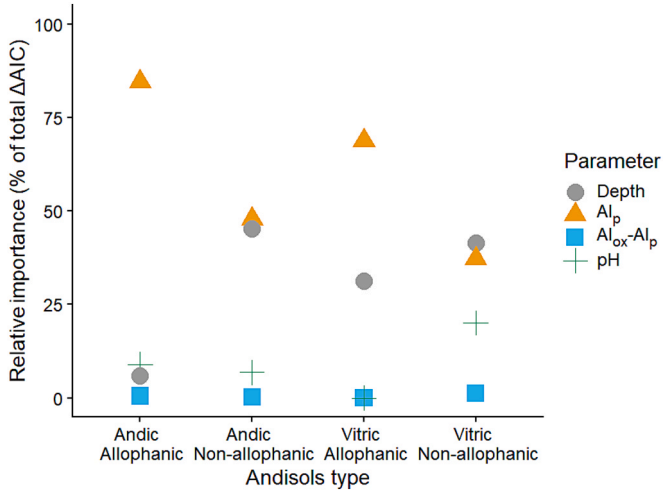

Fig. 8. Variable importance of covariates in generalized additive mixed models (GAMMs) for SOC content, according to the combinations of the soil development stage and dominant reactive Al phases. The random effects are the same as in the main model (see Fig. 4), while only variables shown in the legend are considered.

in Roth-C model was modified by replacing clay content with Al_p to improve the model fitting to the long-term SOC data across Andisols in Japan (Shirato et al., 2004). More recently, in an inventory dataset of Japanese arable topsoils, the phosphate retention capacity, a proxy for reactive Al and Fe contents (Ichinose et al., 2024), explained SOC variation better than clay content across 7500 lowland soils as well as 4300 Andisols (Matsui et al., 2021). These results support broader utility of reactive Al phases to explain SOC variations (see section 4.3).

Our statistical model showed greater importance of Ca_{ex} than Al_p in explaining SOC variation at soil pH >6 (Fig. 6a), which is consistent with the dominance of calcium carbonate control on acid-base reactions in soil exchange complex (Breemen et al., 1983; Chadwick and Chorover, 2001; Rowley et al., 2017). These results align with previous regional- and global-scale studies that have shown the increasing importance of Ca_{ex} in explaining variations in SOC with increasing soil pH (Ichinose et al., 2024; Rasmussen et al., 2018). These trends may be explained by three factors: (i) an increase in soil pH may enhance the liberation of organic ligands from organo-Al complexes, thereby destabilizing them (Takahashi et al., 2006), (ii) an increase in Ca_{ex} associated with higher soil pH may enhance crop productivity and increase carbon input into soil (Heckman et al., 2023; Paradelo et al., 2015), and (iii) an increase in Ca_{ex} may enhance Ca-mediated stabilization of SOC through cation bridging, organo-Ca complexation, and aggregation (Oades, 1988; Rowley et al., 2017). The second factor is unlikely in our case, as there was negative correlation between NPP and Ca_{ex} (Fig. S5). For the third factor, previous studies (Fukumasu et al., 2025; Kaiser et al., 2012) have shown that pyrophosphate extractable organic C (OC) was positively correlated with Ca_{ex} or pyrophosphate extractable Ca in the arable soils with near-neutral pH range, implying that Ca ions may be the dominant form of organo-metal complexes in these soils.

4.2.2. Reactive Al versus Fe phases

We found clear support of the stronger control of Al_p over Fe phases on SOC content (*H1*) using the global Andisols dataset (Fig. 4), which aligns with previous correlation studies across a broad range of soils formed under less-constrained pedogenic conditions (Masiello et al., 2004; Percival et al., 2000; Skjemstad et al., 1990; Wada and Higashi, 1976). Similarly, stronger control of Al_{ox} over Fe_{ox} on SOC content is often observed across soils (e.g., Yu et al., 2021) due possibly to the inclusion of organo-metal complexes in oxalate-extractable pool. Fe phases were relatively more abundant than Al phases outside the Al-buffered pH domain, specifically under strongly acidic conditions for Fe_p and under alkaline, low water availability conditions for SRO Fe minerals (Fig. 5), suggesting a potentially greater role of Fe in SOC persistence under these conditions; however, limited data precluded further assessment. At least three factors may contribute to the greater significance of Al than Fe phases.

First, fundamental chemistry indicates that Al has higher charge density and higher affinity to oxygen-donor ligands such as carboxylic and phenolic functional groups compared to Fe. In soil environments, dissolved Al species can readily form soluble complexes with dissolved organic matter (DOM) holding multiple acidic functional groups (Scheel et al., 2007; Tipping, 2002) whereas dissolved Fe tends to polymerize into colloidal oxides and oxyhydroxides even in the presence of organic acids (Nierop et al., 2002). In fact, reactive Al pools were on average 3.7–3.8 fold greater (on molar basis) than reactive Fe pools (see section 3.2.2). Nevertheless, both metals likely contribute to organo-metal coprecipitate formation in various forms depending on pH, the type of organic matter, and the C:metal ratio (Chen et al., 2023; Kleber et al., 2015).

Second, from a geochemical perspective, Andisol parent materials are commonly dominated by felsic pyroclastic deposits, which generally contain higher Al and lower Fe contents compared to mafic volcanic materials. However, the influence of parent material composition on reactive metal pool sizes is difficult to isolate, because weathering trajectories are strongly influenced by geographic context (see Introduction), the distinction between ash- and lava-derived substrates, and the degree of congruency during mineral dissolution. In particular, mafic minerals tend to release Al and Fe more simultaneously during early weathering, whereas felsic minerals can retain Al in secondary phases (Nesbitt and Young, 1984).

Third, the dominant chemical equilibria governing acid-base reactions in soils (Chadwick and Chorover, 2001; Jackson and Sherman, 1953) predict that dissolved Al tends to occupy cation exchange sites under neutral to moderately acidic pH conditions where most of the Andisols are found (Fig. 2). In contrast, Fe hydrolysis reactions become dominant only under strongly acidic conditions (pH <~4). Thus, at the observed pH range, Al is generally more available than Fe to bind with organic matter unless Fe dissolution from Fe-rich minerals is particularly high. Such exceptions may include non-allophanic soils that have received continental aeolian dust rich in Fe (Inoue and Naruse, 1987; Nagashima et al., 2023).

4.2.3. Organically complexed Al versus SRO Al minerals

Much stronger predictive power of organically complexed Al (Al_p) compared to SRO Al minerals ($Al_{ox} - Al_p$) to explain SOC variation (Fig. 4), even at the pH range favoring allophane and imogolite formation (Dahlgren et al., 2004), is a significant finding as no previous studies have directly demonstrated that Al_p exerts a stronger influence than SRO Al minerals at the global scale. We further found stronger SOC-Al_p relationship in more developed andic Andisols than in vitric ones (Fig. 8), supporting *H2*. Pedogenesis from volcaniclastic materials proceeds from vitric to andic Andisols, and then to other soil orders where reactive metal phases transform into thermodynamically more stable crystalline minerals such as halloysite, kaolinite and gibbsite (Ostwald ripening) (Tadros, 2013). Chronosequence studies (Lawrence et al., 2015; Masiello et al., 2004; Torn et al., 1997) suggest that Al_p, together with other reactive metal phases, may continue to play a critical role for SOC persistence (discussed more in Section 4.3).

Organo-Al complexes estimated by pyrophosphate extraction technique could lead to their overestimation (Parfitt and Childs, 1988; Rennert and Lenhardt, 2024). SRO Al minerals are colloidal in size (Calabi-Floody et al., 2011) and thus susceptible to peptization especially when high-speed centrifugation and/or filtration are omitted in Al_p measurement (Wagai et al., 2013). Thus, further method development to accurately estimate reactive metal phases is critical (Fukumasu et al., 2025; Rennert and Lenhardt, 2024). Nonetheless, distinct pattern of Al_p and Al_{ox}-Al_p against pH (Fig. S10) and the positive correlation between SRO Al and Fe mineral contents (Fig. S5) suggest that this artefact is unlikely to explain the observed patterns.Several factors may explain why Al_p outperformed SRO Al minerals as a predictor of SOC. First, SRO Al minerals have a relatively limited capacity to protect organic matter. Our estimate of allophane content ranged up to 68% (median 4.0%) of the bulk sample mass (Eqs. (1) and (2); Fig. S12). While the amounts of DOM sorbed onto allophane can vary depending on experimental conditions (e.g., solution pH and the molecular composition of DOM used), previous laboratory experiments estimated the maximal adsorption capacity of allophane ranged from 61 to 135 mg C g allophane^{-1} (Ding et al., 2019; Inoue and Wada, 1968). Based on the maximal adsorption capacities, the amount of OC that could be sorptively stabilized by allophane is only 10%−21% of observed SOC (median estimated contribution, n = 1262). Actual contributions of sorptive stabilization by allophane would be even smaller because the maximum DOM adsorption was estimated at a solution pH of 4.5 and the sorptive capacity decreases with increasing pH (Ding et al., 2019), while the median pH of our global dataset was one-unit higher (5.6). A limited importance of sorptive stabilization by SRO Al minerals has been inferred from selective dissolution of various metal phases and co-dissolved organic matter, estimating that only up to 20–30% of total SOC was attributable to sorptive association with SRO Al minerals (allophane/imogolite) in a typical allophanic Andisol (Wagai et al., 2013). These theoretical and experimental estimates support the limited importance of SRO Al mineral in predicting SOC variation, in agreement with our GAMM analysis results (Fig. 4).

Second, organo-Al (and organo-Fe) complexes have a much higher capacity to bind DOM, per mol of metal, compared to sorptive association with SRO Al and Fe minerals (Wagai et al., 2013; Wagai and Mayer, 2007). In our dataset, Al_p:Al_{ox} molar ratios had a median of 0.29 and half of samples ranged from 0.13 to 0.5 (Fig. S11). In other words, the molar mass of Al_p was at least 13% of Al_{ox} for three quarters of the samples. The C:metal molar ratio of organo-metal complexes (pyrophosphate extracts) was previously estimated to be 8.3 for Andisols (i.e. the ratio of pyrophosphate-extractable OC to $Al_p + Fe_p$, Takahashi and Darhgren, 2016). This ratio is more than one order of magnitude higher than that of sorptive associations with SRO Al minerals (Wagai et al., 2013; Wagai and Mayer, 2007). Thus, the observed content of Al_p could account for larger portions of bulk SOC variation than that of Al_{ox}-Al_p phase, even when Al_{ox}-Al_p content was higher.

Soil pH likely alters the stability of organo-metal complexes, despite the consistently strong SOC–Al_p relationship across the pH gradient below ~6.5 (Fig. 4; Fig. 6a). The higher abundance of Al_p and Fe_p relative to SRO Al and Fe minerals at pH < ~5 (Fig. S11a,b) can be attributed to the high affinity of organic ligands for metals, which enhances resistance of associated C to microbial degradation and suppresses SRO mineral formation (Boudot et al., 1989; Kunito et al., 2016; Scheel et al., 2008). Because the dominant metal-binding functional groups in soil organic matter—primarily carboxyl groups—have apparent pKa values around pH 4–5, with broader distributions extending to ~6 (Sparks, 2003; Tipping, 2002), decreasing pH promotes ligand protonation, which weakens metal–ligand bonding and increases free Al^{3+} activity. However, the resulting increase in potential ligand biodegradability is likely offset by reduced microbial and enzymatic activity under strongly acidic, Al-toxic conditions. At moderately acidic

pH (5–6.5), stronger inner-sphere and polydentate metal–organic bonding enhances the stability of organo-metal complexes, thereby limiting SRO mineral formation even though Al and Fe hydroxides exhibit minimum solubility in this pH range.

Precipitation of organo-Al complexes may outpace their re-dissolution, promoting shifts in Al speciation and contributing to their persistence. In Andisols, exchangeable, organically complexed, and polymerized Al phases (e.g., SRO aluminosilicates) coexist under dynamic equilibrium (Dahlgren et al., 2004; Mizota and Reeuwijk, 1989), a framework that may also apply to other soils at lower Al contents. Precipitation of dissolved organo-metal complexes can occur during metastable supersaturation or drying, and coprecipitation with other metals (e.g., Ca, Fe, Mn) or with colloidal clays and metal oxides likely enhances resistance to dissolution and microbial degradation. When precipitation exceeds re-dissolution, Al is redistributed from less reactive mineral reservoirs, potentially expanding the operationally defined reactive Al pool over pedogenic timescales. Although speculative, these processes may explain the persistence of organo-Al complexes in older, non-allophanic Andisols and potentially in a broader range of soils (Lawrence et al., 2015; Percival et al., 2000).

In summary, although Al_p was the strongest overall predictor of SOC, its dominance varied systematically with pedogenic conditions. Strongly acidic soils (pH ~4–5) favored Al_p over SRO Al minerals (Al_{ox}–Al_p, Fig. S11a), whereas moderately acidic soils (pH ~5–6) promoted the coexistence of Al_p and Al_{ox}–Al_p pools (Fig. S10a, c). Across this range, organo-Al complexes exerted the primary control on SOC variation (Fig. 6a). In contrast, more alkaline and drier conditions (pH > ~6.5) depleted reactive Al pools (Fig. S10a, c) and shifted soils towards carbonate-buffered systems (section 4.1), under which exchangeable Ca became more important for SOC storage (Fig. 6a). Together, these results support *H3*.

4.3. Global significance of organo-Al complexation beyond Andisols

Pyrophosphate-extractable Al (Alp) is widely recognized as a strong correlate of soil C in volcanic soils, reflecting the stabilizing role of organo–Al complexes. Under very acidic conditions, large proportions of Al are associated with organic matter, while inorganic Al phases remain abundant. At moderately acidic pH (~4.5–6.5), continuous Al supply from SRO Al minerals and strong complexation by organic ligands (Section 4.1) maintain low free Al^{3+} activity and favor organo-Al dominance. Although these reactions are especially pronounced in Andisols, they arise from general water flux–driven pedogenesis and thus occur across soil types (Chadwick and Chorover, 2001). Consequently, while global-scale studies tend to emphasize the protective role of SRO Al and Fe minerals for SOC across a range of soil types under moderately acidic and wet conditions, particularly at depth (von Fromm et al., 2025; Rasmussen et al., 2018), our results indicate that organo–Al complexation may dominate SOC stabilization across much of the pH range below ~6.5 in a broad array of soils.

The consistently stronger predictive power of Al_p relative to SRO Al minerals, reactive Fe phases, or soil texture highlights the importance of organically complexed Al pool for explaining SOC variation. Our global analysis, together with prior findings that clay or clay + silt contents are much weaker predictors of SOC than reactive Al pools across a wide range of soil types under humid climates (Section 4.2.1), suggests that reactive Al content can provide a more robust basis than texture for soils' potential capacity to stabilize SOC. This has direct implications for modeling, as most soil C models rely on texture-based modifiers (%clay) to parameterize mineral protection, while largely omitting explicit representations of reactive Al and Fe phases (Bailey et al., 2018; Basile-Doelsch et al., 2020).

Identifying dominant SOC stabilization mechanisms remains critical because alternative mechanisms imply fundamentally different representations in SOC models. Regional- to global-scale correlations between SOC and oxalate-extractable metals (von Fromm et al., 2025; Ren et al., 2024; Yu et al., 2021) are commonly interpreted as sorptive stabilization by SRO minerals, often characterized by non-linear SOC increases and apparent saturation behavior (Yu et al., 2021) analogous to texture-based limits (Georgiou et al., 2025). These patterns are typically attributed to saturation of mineral protective capacity or limitations in C inputs. In contrast, our Andisol dataset which covers equally broad climatic gradients while constraining parent material and soil age showed largely linear SOC responses to increasing Al_p and SRO Al mineral contents (Fig. 4). This contrast suggests that, where reactive metal supply is sustained by weathering, SOC storage and organo-metal complex formation may be governed by the balance between metal and carbon inputs rather than by fixed mineral saturation limits or C supply alone.

Stoichiometric considerations support this interpretation and further imply the importance of reactive metal supply. Typical C/metal molar ratio of the organo-metal complexes is 8.3 (Takahashi and Dahlgren, 2016), whereas bulk SOC/Al_p ratio in our dataset mostly ranged between 9 and 15 (median 13.5, interquartile range 8.5–14.6, n = 1689, Fig. S2), consistent with values reported for tropical weathered soils (SOC/(Al_p + Fe_p) ratio of 12–17 in A horizons and 5–8 in B horizons; Ashida et al., (2021)). While bulk SOC includes particulate OM not primarily associated with metals, *meso*-density fraction (isolated by sequential density fractionation) represents the main mineral-associated SOC pool. Interestingly, C/Al_p ratio in these fractions was even higher, 17.8 ± 3.5 among soils from five soil orders (Wagai et al., 2020), in agreement with previous studies (Heckman et al., 2018; Wagai et al., 2013). These results suggest that Al released through ion exchange or weathering is efficiently complexed by organic ligands (Berggren and Mulder, 1995; Heckman et al., 2013), consistent with a strong role of reactive metal availability in organo-metal complex formation.

As the most practical index of the reactive Al pool at regional to global scales, we propose the use of Al_{ox}. First, Al_{ox} pool includes both organically complexed Al (Al_p) and SRO Al minerals, thereby serving as an integrated proxy for reactive Al. Second, Al_{ox} measurements are far more widely available than Al_p in global datasets (von Fromm et al., 2025). Third, reactive Al and Fe phases—including organo-Al complexes and SRO Al and Fe minerals, and to a limited extent, crystalline metal oxides—may act synergistically to enhance SOC persistence via coprecipitation-type processes including ternary association of Al^{3+}, dissolved organic matter, and oligomeric precursors of SRO minerals (Jamoteau et al., 2024; Tamrat et al., 2019; Wagai et al., 2020), as well as through microaggregate formation involving other metals (e.g., Ca), clay minerals, and organic or inorganic binding agents (Amelung et al., 2023; Totsche et al., 2018; Wagai and Mayer, 2007). For example, SOC showed a strong linear relationship with Al_p + Fe_p across both young and old (buried) Andisol horizons in Japan, whereas associations with hydrous Al and Fe oxides, including SRO minerals, became pronounced only after 2.5–5 kyr of burial (Wada and Higashi, 1976). Consistent with this, Lawrence et al. (2015) demonstrated that Al_p and Fe_p, in combination with high surface area secondary minerals such as halloysite, best explain the variation in SOC storage and persistence along a 0.25–1200 kyr chronosequence under a wet, temperate climate (Lawrence et al., 2015). These findings indicate that multiple metal-mediated stabilization mechanisms can operate concurrently, with shifting dominance over pedogenic timescales as soil pH buffering domains evolve.

In this context, Al_{ox} could serve as a useful surrogate for the suite of reactive metal phases, supported by (i) predictable changes in relative abundance of Al_p and Al_{ox} along soil pH gradient (Fig. S11a), and (ii) generally systematic changes in reactive Al and Fe speciation patterns (Al_p/Al_{ox} and Fe_p/Fe_{ox} ratios) against soil pH and MAP–PET (Fig. S11). Nevertheless, the use of Al_{ox} as a proxy for SOC protection hinges on improved mechanistic understanding of how reactive metal pools form, transform, and interact with organic matter across multiple timescales, from management-relevant annual to decadal scales to longer pedogenic timescales. Such understanding is important for informing SOC models that seek to represent mineral-associated carbon persistence. Progress

toward this goal will require improved representation of coupled weathering and biogeochemical processes governing organo–mineral interactions.

CRediT authorship contribution statement

Morimaru Kida: Writing – review & editing, Writing – original draft, Software, Project administration, Methodology, Funding acquisition, Formal analysis, Data curation, Conceptualization. **Hirohiko Nagano:** Writing – review & editing, Software, Funding acquisition, Data curation, Conceptualization. **Hiroaki Shimada:** Writing – review & editing, Data curation, Conceptualization. **Jumpei Fukumasu:** Writing – review & editing, Data curation, Conceptualization. **Rota Wagai:** Writing – review & editing, Project administration, Funding acquisition, Conceptualization.

Declaration of competing interest

The authors declare no competing interests.

Acknowledgements

We are grateful to Tadashi Takahashi at Akita Prefectural University and Masami Nanzyo (Emeritus Professor) at Tohoku University for the access to TUWAD. We also thank Noriko Yamaguchi for valuable discussion on aluminum chemistry. This study was supported by startup funding from Kobe University (M.K.) and JSPS KAKENHI Grant Numbers JP24H01513 (M.K.), JP25K03249 (M.K.), JP21H02231 (H.N.), JP22H05717 (H.N.), and JP21H03580 (R.W.)

Appendix A. Supplementary material

Supplementary data to this article can be found online at https://doi.org/10.1016/j.geoderma.2026.117740.

Data availability

The dataset is freely available at PANGAEA URL: https://doi.pangaea.de/10.1594/PANGAEA.977631).

References

Abatzoglou, J.T., Dobrowski, S.Z., Parks, S.A., Hegewisch, K.C., 2018. TerraClimate, a high-resolution global dataset of monthly climate and climatic water balance from 1958–2015. Sci. Data 5, 170191. https://doi.org/10.1038/sdata.2017.191.

Alam, M.M., Yamakita, E., Inoue, Y., Koarashi, J., Atarashi-Andoh, M., Abe, Y., Nakayama, M., Mori, Y., Hiradate, S., 2025. Possible transition from Silandic to Aluandic Andosols with acidification as evidenced by detailed profile investigation of two well-preserved forest Andosols in Japan. Soil Sci. Plant Nutr. 1–12. https://doi.org/10.1080/00380768.2025.2511803.

Amelung, W., Meyer, N., Rodionov, A., Knief, C., Aehnelt, M., Bauke, S.L., Biesgen, D., Dultz, S., Guggenberger, G., Jaber, M., Klumpp, E., Kögel-Knabner, I., Nischwitz, V., Schweizer, S.A., Wu, B., Totsche, K.U., Lehndorff, E., 2023. Process sequence of soil aggregate formation disentangled through multi-isotope labelling. Geoderma 429, 116226. https://doi.org/10.1016/j.geoderma.2022.116226.

Arai, M., Ikazaki, K., Anzai, T., Celestial, V.P., Tumbay, J.V., Santillana, I.S., Wagai, R., 2025. Protective role of reactive aluminum phases to stabilize soil organic matter against long-term cultivation in the humid tropics under volcanic influence. Soil Sci. Plant Nutr. 71, 27–37. https://doi.org/10.1080/00380768.2024.2415455.

Arnalds, O., 2004. Volcanic soils of Iceland. Catena 56, 3–20. https://doi.org/10.1016/j.catena.2003.10.002.

Asano, M., Wagai, R., 2014. Evidence of aggregate hierarchy at micro- to submicron scales in an allophanic Andisol. Geoderma 216, 62–74. https://doi.org/10.1016/j.geoderma.2013.10.005.

Ashida, K., Watanabe, T., Urayama, S., Hartono, A., Kilasara, M., Ze, A.D.M., Nakao, A., Sugihara, S., Funakawa, S., 2021. Quantitative relationship between organic carbon and geochemical properties in tropical surface and subsurface soils. Biogeochemistry 155, 77–95. https://doi.org/10.1007/s10533-021-00813-8.

Bailey, V.L., Bond-Lamberty, B., DeAngelis, K., Grandy, A.S., Hawkes, C.V., Heckman, K., Lajtha, K., Phillips, R.P., Sulman, B.N., Todd-Brown, K.E.O., Wallenstein, M.D., 2018. Soil carbon cycling proxies: Understanding their critical role in predicting climate change feedbacks. Glob. Chang. Biol. 24, 895–905. https://doi.org/10.1111/gcb.13926.

Baldock, J., Skjemstad, J., 2000. Role of the soil matrix and minerals in protecting natural organic materials against biological attack. Org Geochem. 31, 697–710. https://doi.org/10.1016/s0146-6380(00)00049-8.

Basile-Doelsch, I., Balesdent, J., Pellerin, S., 2020. Reviews and syntheses: the mechanisms underlying carbon storage in soil. Biogeosciences 17, 5223–5242. https://doi.org/10.5194/bg-17-5223-2020.

Berggren, D., Mulder, J., 1995. The role of organic matter in controlling aluminum solubility in acidic mineral soil horizons. Geochim. Cosmochim. Acta 59, 4167–4180. https://doi.org/10.1016/0016-7037(95)94443-j.

Boudot, J.P., Hadj, A.B., Steiman, R., Seigle-Murandi, F., 1989. Biodegradation of synthetic organo-metallic complexes of iron and aluminium with selected metal to carbon ratios. Soil Biol. Biochem. 21, 961–966. https://doi.org/10.1016/0038-0717(89)90088-6.

van Breemen, N., Mulder, J., Driscoll, C.T., 1983. Acidification and alkalinization of soils. Plant Soil 75, 283–308. https://doi.org/10.1007/bf02369968.

Buchhorn, M., Lesiv, M., Tsendbazar, N.-E., Herold, M., Bertels, L., Smets, B., 2020. Copernicus global land cover layers—collection 2. Remote Sens.-Basel 12, 1044. https://doi.org/10.3390/rs12061044.

Calabi-Floody, M., Bendall, J.S., Jara, A.A., Welland, M.E., Theng, B.K.G., Rumpel, C., de la Mora, M.L., 2011. Nanoclays from an Andisol: extraction, properties and carbon stabilization. Geoderma 161, 159–167. https://doi.org/10.1016/j.geoderma.2010.12.013.

Chadwick, O.A., Chorover, J., 2001. The chemistry of pedogenic thresholds. Geoderma 100, 321–353. https://doi.org/10.1016/s0016-7061(01)00027-1.

Chen, K.-Y., Liu, Y.-T., Hung, J.-T., Hsieh, Y.-C., Tzou, Y.-M., 2023. Synergism of Fe and Al salts for the coagulation of dissolved organic matter: structural developments of Fe/Al-organic matter associations. Chemosphere 316, 137737. https://doi.org/10.1016/j.chemosphere.2023.137737.

Dahlgren, R.A., Saigusa, M., Ugolini, F.C., 2004. The nature, properties and management of volcanic soils. Adv. Agron. 82, 113–182. https://doi.org/10.1016/s0065-2113(03)82003-5.

Delmelle, P., Opfergelt, S., Cornelis, J.-T., Ping, C.-L., 2015. The encyclopedia of volcanoes. In: Part IX: Econ. Benefits Cult. Asp. Volcanism, second ed., pp. 1253–1264. https://doi.org/10.1016/b978-0-12-385938-9.00072-9.

Ding, Y., Lu, Y., Liao, P., Peng, S., Liang, Y., Lin, Z., Dang, Z., Shi, Z., 2019. Molecular fractionation and sub-nanoscale distribution of dissolved organic matter on allophane. Environ. Sci. Nano 6, 2037–2048. https://doi.org/10.1039/c9en00335e.

Egli, M., Nater, M., Mirabella, A., Raimondi, S., Plötze, M., Alioth, L., 2008. Clay minerals, oxyhydroxide formation, element leaching and humus development in volcanic soils. Geoderma 143, 101–114. https://doi.org/10.1016/j.geoderma.2007.10.020.

Eguchi, T., Tanaka, R., Maejima, Y., Tamura, K., 2012. The influence of aeolian dust in non-allophanic Andosols on Yakushima Island. Soil Sci. Plant Nutr. 58, 191–199. https://doi.org/10.1080/00380768.2012.672926.

von Fromm, S.F., Doetterl, S., Butler, B.M., Aynekulu, E., Berhe, A.A., Haefele, S.M., McGrath, S.P., Shepherd, K.D., Six, J., Tamene, L., Tondoh, E.J., Vågen, T., Winowiecki, L.A., Trumbore, S.E., Hoyt, A.M., 2024. Controls on timescales of soil organic carbon persistence across sub-Saharan Africa. Glob. Chang. Biol. 30, e17089. https://doi.org/10.1111/gcb.17089.

von Fromm, S.F., Hoyt, A.M., Lange, M., Acquah, G.E., Aynekulu, E., Berhe, A.A., Haefele, S.M., McGrath, S.P., Shepherd, K.D., Sila, A.M., Six, J., Towett, E.K., Trumbore, S.E., Vågen, T.-G., Weullow, E., Winowiecki, L.A., Doetterl, S., 2021. Continental-scale controls on soil organic carbon across sub-Saharan Africa. Soil 7, 305–332. https://doi.org/10.5194/soil-7-305-2021.

von Fromm, S.F., Jungkunst, H.F., Amenkhienan, B., Hall, S.J., Georgiou, K., Pries, C.H., Montaño-López, F., Quesada, C.A., Rasmussen, C., Schrumpf, M., Singh, B., Thompson, A., Wagai, R., Fiedler, S., 2025. Moisture and soil depth govern relationships between soil organic carbon and oxalate-extractable metals at the global scale. Biogeochemistry 168, 20. https://doi.org/10.1007/s10533-025-01208-9.

Fukumasu, J., Poeplau, C., Coucheney, E., Jarvis, N., Klöffel, T., Koestel, J., Kätterer, T., Svensson, D.N., Wetterlind, J., Larsbo, M., 2021. Oxalate-extractable aluminum alongside carbon inputs may be a major determinant for organic carbon content in agricultural topsoils in humid continental climate. Geoderma 402, 115345. https://doi.org/10.1016/j.geoderma.2021.115345.

Fukumasu, J., Yang, P.-T., Kajiura, M., Gregorich, E., Wagai, R., 2025. Soil extraction with pyrophosphate-dithionite mixture: a practical method to estimate organic carbon associated with metal cations and reactive mineral phases. Soil Sci. Plant Nutr. 1–13. https://doi.org/10.1080/00380768.2024.2448861.

Georgiou, K., Angers, D., Champiny, R.E., Cotrufo, M.F., Craig, M.E., Doetterl, S., Grandy, A.S., Lavallee, J.M., Lin, Y., Lugato, E., Poeplau, C., Rocci, K.S., Schweizer, S.A., Six, J., Wieder, W.R., 2025. Soil carbon saturation: what do we really know? Glob. Chang. Biol. 31, e70197. https://doi.org/10.1111/gcb.70197.

Hall, S.J., Thompson, A., 2022. What do relationships between extractable metals and soil organic carbon concentrations mean? Soil Sci. Soc. Am. J. https://doi.org/10.1002/saj2.20343.

Hassink, J., 1997. The capacity of soils to preserve organic C and N by their association with clay and silt particles. Plant Soil 191, 77–87. https://doi.org/10.1023/a:1004213929699.

Heckman, K., Grandy, A., Gao, X., Keiluweit, M., Wickings, K., Carpenter, K., Chorover, J., Rasmussen, C., 2013. Sorptive fractionation of organic matter and formation of organo-hydroxy-aluminum complexes during litter biodegradation in the presence of gibbsite. Geochim. Cosmochim. Acta 121, 667–683. https://doi.org/10.1016/j.gca.2013.07.043.

Heckman, K., Lawrence, C.R., Harden, J.W., 2018. A sequential selective dissolution method to quantify storage and stability of organic carbon associated with Al and Fe

hydroxide phases. Geoderma 312, 24–35. https://doi.org/10.1016/j.geoderma.2017.09.043.
Heckman, K., Pries, C.E.H., Lawrence, C.R., Rasmussen, C., Crow, S.E., Hoyt, A.M., von Fromm, S.F., Shi, Z., Stoner, S., McGrath, C., Beem-Miller, J., Berhe, A.A., Blankinship, J.C., Keiluweit, M., Marín-Spiotta, E., Monroe, J.G., Plante, A.F., Schimel, J., Sierra, C.A., Thompson, A., Wagai, R., 2021. Beyond bulk: density fractions explain heterogeneity in global soil carbon abundance and persistence. Glob. Chang. Biol. https://doi.org/10.1111/gcb.16023.
Heckman, K.A., Possinger, A.R., Badgley, B.D., Bowman, M.M., Gallo, A.C., Hatten, J.A., Nave, L.E., SanClements, M.D., Swanston, C.W., Weiglein, T.L., Wieder, W.R., Strahm, B.D., 2023. Moisture-driven divergence in mineral-associated soil carbon persistence. Proc. Natl. Acad. Sci. 120, e2210044120. https://doi.org/10.1073/pnas.2210044120.
Ichinose, Y., Matsui, K., Fukumasu, J., Matsuura, S., Takata, Y., Wagai, R., 2024. How do reactive aluminum and iron phases control soil organic carbon and phosphate adsorption capacity in agricultural topsoils across Japan? Soil Sci. Plant Nutr. 1–15. https://doi.org/10.1080/00380768.2024.2410322.
Inoue, K., Naruse, T., 2009. Asian long-range eolian dust deposited on soils and paleosols along the Japan Sea coast. Quat. Res. Daiyonki-Kenkyu) 29, 209. https://doi.org/10.4116/jaqua.29.209.
Inoue, K., Naruse, T., 1987. Physical, chemical, and mineralogical characteristics of modern eolian dust in Japan and rate of dust deposition. Soil Sci. Plant Nutr. 33, 327–345. https://doi.org/10.1080/00380768.1987.10557579.
Inoue, T., Wada, K., 1968. Adsorption of humified clover extracts by various clays. In: ISSS, 9th International Congress of Soil Science Transactions, pp. 289–298.
IUSS Working Group WRB, 2015. World Reference Base (WRB) for Soil Resources 2014 (International soil classification system for naming soils and creating legends for soil maps), World Soil Resources Reports. FAO, Rome. https://doi.org/10.1108/09504121011021959.
Jackson, M.L., Sherman, G.D., 1953. Chemical weathering of minerals in soils. Adv. Agron. 5, 219–318. https://doi.org/10.1016/s0065-2113(08)60231-x.
Jamoteau, F., Doelsch, E., Cam, N., Levard, C., Woignier, T., Boulineau, A., Saint-Antonin, F., Swaraj, S., Gassier, G., Duvivier, A., Borschneck, D., Pons, M.-L., Chaurand, P., Vidal, V., Brouilly, N., Basile-Doelsch, I., 2024. Cultivation reduces quantities of mineral-organic associations in the form of amorphous coprecipitates. Egusphere 2024, 1–22. https://doi.org/10.5194/egusphere-2024-2933.
Jansen, B., Nierop, K.G.J., Verstraten, J.M., 2003. Mobility of Fe(II), Fe(III) and Al in acidic forest soils mediated by dissolved organic matter: influence of solution pH and metal/organic carbon ratios. Geoderma 113, 323–340. https://doi.org/10.1016/s0016-7061(02)00368-3.
Jenny, H., 1941. Factors of Soil Formation: A System of Quantitative Pedology. McGraw-Hill Book Company, New York.
Kaiser, M., Ellerbrock, R.H., Wulf, M., Dultz, S., Hierath, C., Sommer, M., 2012. The influence of mineral characteristics on organic matter content, composition, and stability of topsoils under long-term arable and forest land use. J. Geophys. Res. Biogeosciences 117. https://doi.org/10.1029/2011jg001712.
Kida, M., Shimada, H., Nagano, H., Fukumasu, J., Wagai, R., 2025. Refined estimates of organic carbon stocks in global Andisols. Soil Sci. Plant Nutr. 1–5. https://doi.org/10.1080/00380768.2025.2603931.
Kleber, M., Eusterhues, K., Keiluweit, M., Mikutta, C., Mikutta, R., Nico, P.S., 2015. Chapter one mineral–organic associations: formation, properties, and relevance in soil environments. Adv. Agron. 130, 1–140. https://doi.org/10.1016/bs.agron.2014.10.005.
Klotzbücher, T., Treptow, C., Kaiser, K., Klotzbücher, A., Mikutta, R., 2020. Sorption competition with natural organic matter as mechanism controlling silicon mobility in soil. Sci. Rep. 10, 11225. https://doi.org/10.1038/s41598-020-68042-x.
Kunito, T., Isomura, I., Sumi, H., Park, H.-D., Toda, H., Otsuka, S., Nagaoka, K., Saeki, K., Senoo, K., 2016. Aluminum and acidity suppress microbial activity and biomass in acidic forest soils. Soil Biol. Biochem. 97, 23–30. https://doi.org/10.1016/j.soilbio.2016.02.019.
Lavallee, J.M., Soong, J.L., Cotrufo, M.F., 2020. Conceptualizing soil organic matter into particulate and mineral-associated forms to address global change in the 21st century. Glob. Chang. Biol. 26, 261–273. https://doi.org/10.1111/gcb.14859.
Lawrence, C.R., Harden, J.W., Xu, X., Schulz, M.S., Trumbore, S.E., 2015. Long-term controls on soil organic carbon with depth and time: a case study from the Cowlitz River Chronosequence, WA USA. Geoderma 247–248, 73–87. https://doi.org/10.1016/j.geoderma.2015.02.005.
Lettens, S., Vos, B.D., Quataert, P., Wesemael, B.V., Muys, B., Orshoven, J.V., 2007. Variable carbon recovery of Walkley-Black analysis and implications for national soil organic carbon accounting. Eur. J. Soil Sci. 58, 1244–1253. https://doi.org/10.1111/j.1365-2389.2007.00916.x.
Lilienfein, J., Qualls, R.G., Uselman, S.M., Bridgham, S.D., 2003. Soil formation and organic matter accretion in a young andesitic chronosequence at Mt. Shasta, California. Geoderma 116, 249–264. https://doi.org/10.1016/s0016-7061(03)00086-7.
Lyu, H., Watanabe, T., Kilasara, M., Hartono, A., Funakawa, S., 2021. Soil organic carbon pools controlled by climate and geochemistry in tropical volcanic regions. Sci. Total Environ. 761, 143277. https://doi.org/10.1016/j.scitotenv.2020.143277.
Masiello, C.A., Chadwick, O.A., Southon, J., Torn, M.S., Harden, J.W., 2004. Weathering controls on mechanisms of carbon storage in grassland soils. Global Biogeochem. Cycles 18, n/a-n/a. https://doi.org/10.1029/2004gb002219.
Matsui, K., Takata, Y., Matsuura, S., Wagai, R., 2021. Soil organic carbon was more strongly linked with soil phosphate fixing capacity than with clay content across 20,000 agricultural soils in Japan: a potential role of reactive aluminum revealed by soil database approach. Soil Sci. Plant Nutr. 1–10. https://doi.org/10.1080/00380768.2021.1902750.
Matus, F., Amigo, X., Kristiansen, S.M., 2006. Aluminium stabilization controls organic carbon levels in Chilean volcanic soils. Geoderma 132, 158–168. https://doi.org/10.1016/j.geoderma.2005.05.005.
Matus, F., Garrido, E., Sepúlveda, N., Cárcamo, I., Panichini, M., Zagal, E., 2008. Relationship between extractable Al and organic C in volcanic soils of Chile. Geoderma 148, 180–188. https://doi.org/10.1016/j.geoderma.2008.10.004.
Matus, F., Rumpel, C., Neculman, R., Panichini, M., Mora, M.L., 2014. Soil carbon storage and stabilisation in andic soils: a review. Catena 120, 102–110. https://doi.org/10.1016/j.catena.2014.04.008.
Matus, F.J., 2025. Mineral-associated carbon persistence arises from steady-state dynamics, not saturation. Soil Sci. Plant Nutr. 1–11. https://doi.org/10.1080/00380768.2025.2595442.
McNally, S.R., Beare, M.H., Curtin, D., Meenken, E.D., Kelliher, F.M., Pereira, R.C., Shen, Q., Baldock, J., 2017. Soil carbon sequestration potential of permanent pasture and continuous cropping soils in New Zealand. Glob. Chang. Biol. 23, 4544–4555. https://doi.org/10.1111/gcb.13720.
Mikutta, R., Schaumann, G.E., Gildemeister, D., Bonneville, S., Kramer, M.G., Chorover, J., Chadwick, O.A., Guggenberger, G., 2009. Biogeochemistry of mineral–organic associations across a long-term mineralogical soil gradient (0.3–4100kyr), Hawaiian Islands. Geochim. Cosmochim. Acta 73, 2034–2060. https://doi.org/10.1016/j.gca.2008.12.028.
Mizota, C., van Reeuwijk, L.P., 1989. Clay mineralogy and chemistry of soil formed in volcanic materials in diverse climatic regions. Soil Monogr. 2.
Nagashima, K., Kawakami, H., Sugie, K., Fujiki, T., Nishioka, J., Iwamoto, Y., Takemura, T., Miyakawa, T., Taketani, F., Aita, M.N., 2023. Asian dust-deposition flux to the subarctic Pacific estimated using single quartz particles. Sci. Rep. 13, 15424. https://doi.org/10.1038/s41598-023-41201-6.
Nanzyo, M., Shoji, S., Dahlgren, R., 1993. Chapter 7 physical characteristics of volcanic ash soils. Dev. Soil Sci. 21, 189–207. https://doi.org/10.1016/s0166-2481(08)70268-x.
Nesbitt, H.W., Young, G.M., 1984. Prediction of some weathering trends of plutonic and volcanic rocks based on thermodynamic and kinetic considerations. Geochim. Cosmochim. Acta 48, 1523–1534. https://doi.org/10.1016/0016-7037(84)90408-3.
Nierop, K.G., Jansen, B., Verstraten, J.M., 2002. Dissolved organic matter, aluminium and iron interactions: precipitation induced by metal/carbon ratio, pH and competition. Sci. Total Environ. 300, 201–211. https://doi.org/10.1016/s0048-9697(02)00254-1.
Oades, J., 1988. The retention of organic matter in soils. Biogeochemistry 5, 35–70. https://doi.org/10.1007/bf02180317.
Paradelo, R., Virto, I., Chenu, C., 2015. Net effect of liming on soil organic carbon stocks: a review. Agric. Ecosyst. Environ. 202, 98–107. https://doi.org/10.1016/j.agee.2015.01.005.
Parfitt, R., Childs, C., 1988. Estimation of forms of Fe and Al – a review, and analysis of contrasting soils by dissolution and Mossbauer methods. Soil Res. 26, 121–144. https://doi.org/10.1071/sr9880121.
Parfitt, R.L., 2009. Allophane and imogolite: role in soil biogeochemical processes. Clay Miner. 44, 135–155. https://doi.org/10.1180/claymin.2009.044.1.135.
Parfitt, R.L., 1990. Allophane in New Zealand – a review. Soil Res. 28, 343–360. https://doi.org/10.1071/sr9900343.
Parton, W.J., Schimel, D.S., Cole, C.V., Ojima, D.S., 1987. Analysis of factors controlling soil organic matter levels in great plains grasslands. Soil Sci. Soc. Am. J. 51, 1173–1179. https://doi.org/10.2136/sssaj1987.03615995005100050015x.
Peña-Ramírez, V.M., Vázquez-Selem, L., Siebe, C., 2009. Soil organic carbon stocks and forest productivity in volcanic ash soils of different age (1835–30,500 years B.P.) in Mexico. Geoderma 149, 224–234. https://doi.org/10.1016/j.geoderma.2008.11.038.
Percival, H.J., Parfitt, R.L., Scott, N.A., 2000. Factors controlling soil carbon levels in new zealand grasslands is clay content important? Soil Sci. Soc. Am. J. 64, 1623–1630. https://doi.org/10.2136/sssaj2000.6451623x.
Ping, C.L., Shoji, S., Ito, T., 1988. Properties and classification of three volcanic ash-derived pedons from Aleutian Islands and Alaska Peninsula, Alaska. Soil Sci. Soc. Am. J. 52, 455–462. https://doi.org/10.2136/sssaj1988.03615995005200020028x.
Rasmussen, C., Heckman, K., Wieder, W.R., Keiluweit, M., Lawrence, C.R., Berhe, A.A., Blankinship, J.C., Crow, S.E., Druhan, J.L., Pries, C.E.H., Marin-Spiotta, E., Plante, A. F., Schädel, C., Schimel, J.P., Sierra, C.A., Thompson, A., Wagai, R., 2018. Beyond clay: towards an improved set of variables for predicting soil organic matter content. Biogeochemistry 137, 297–306. https://doi.org/10.1007/s10533-018-0424-3.
Ren, S., Wang, C., Zhou, Z., 2024. Global distributions of reactive iron and aluminum influence the spatial variation of soil organic carbon. Glob. Chang. Biol. 30, e17576. https://doi.org/10.1111/gcb.17576.
Rennert, T., 2018. Wet-chemical extractions to characterise pedogenic Al and Fe species – a critical review. Soil Res. 57, 1. https://doi.org/10.1071/sr18299.
Rennert, T., Lenhardt, K.R., 2024. Potential pitfalls when using popular chemical extractions to characterize Al- and Fe-containing soil constituents. J. Plant Nutr. Soil Sci. https://doi.org/10.1002/jpln.202300268.
Rowley, M.C., Grand, S., Verrecchia, É.P., 2017. Calcium-mediated stabilisation of soil organic carbon. Biogeochemistry 137, 27–49. https://doi.org/10.1007/s10533-017-0410-1.
Running, S., Zhao, M., 2021. In: MODIS/Terra Net Primary Production Gap-Filled Yearly L4 Global 500m SIN Grid V061. NASA EOSDIS Land Processes Distributed Active Archive Center. https://doi.org/10.5067/modis/mod17a3hgf.061.
Salonen, A., de Goede, R., Creamer, R., Heinonsalo, J., Soinne, H., 2024. Soil organic carbon fractions and storage potential in Finnish arable soils. Eur. J. Soil Sci. 75. https://doi.org/10.1111/ejss.13527.
Sato, H.H., Ikeda, W., Paeth, R., Smythe, R., Takehiro, M., 1973. Soil survey of the Island of Hawaii, State of Hawaii. U.S. Govt. Print. Off.

Scheel, T., Dörfler, C., Kalbitz, K., 2007. Precipitation of dissolved organic matter by aluminum stabilizes carbon in acidic forest soils. Soil Sci. Soc. Am. J. 71, 64–74. https://doi.org/10.2136/sssaj2006.0111.
Scheel, T., Jansen, B., Wijk, A.J.V., Verstraten, J.M., Kalbitz, K., 2008. Stabilization of dissolved organic matter by aluminium: a toxic effect or stabilization through precipitation? Eur. J. Soil Sci. 59, 1122–1132. https://doi.org/10.1111/j.1365-2389.2008.01074.x.
Schmidt, M.W.I., Torn, M.S., Abiven, S., Dittmar, T., Guggenberger, G., Janssens, I.A., Kleber, M., Kögel-Knabner, I., Lehmann, J., Manning, D.A.C., Nannipieri, P., Rasse, D.P., Weiner, S., Trumbore, S.E., 2011. Persistence of soil organic matter as an ecosystem property. Nature 478, 49–56. https://doi.org/10.1038/nature10386.
Shirato, Y., Hakamata, T., Taniyama, I., 2004. Modified rothamsted carbon model for andosols and its validation: changing humus decomposition rate constant with pyrophosphate-extractable Al. Soil Sci. Plant Nutr. 50, 149–158. https://doi.org/10.1080/00380768.2004.10408463.
Shoji, S., 1985. Genesis and properties of non-allophanic andisols in Japan. Appl. Clay Sci. 1, 83–88. https://doi.org/10.1016/0169-1317(85)90564-2.
Shoji, S., Dahlgren, R., Nanzyo, M., 1993. Chapter 3 Genesis of volcanic ash soils. Dev. Soil Sci. 21, 37–71. https://doi.org/10.1016/s0166-2481(08)70264-2.
Shoji, S., Nanzyo, M., Dahlgren, R.A., Quantin, P., 1996. Evaluation and proposed revisions of criteria for Andosols in the World Reference Base for Soil Resources. Soil Sci. 161, 604–615. https://doi.org/10.1097/00010694-199609000-00005.
Silva, J.H.S., Deenik, J.L., Yost, R.S., Bruland, G.L., Crow, S.E., 2015. Improving clay content measurement in oxidic and volcanic ash soils of Hawaii by increasing dispersant concentration and ultrasonic energy levels. Geoderma 237, 211–223. https://doi.org/10.1016/j.geoderma.2014.09.008.
Simpson, G.L., 2023. gratia: Graceful ggplot-Based Graphics and Other Functions for GAMs Fitted Using mgcv.
Six, J., Conant, R.T., Paul, E.A., Paustian, K., 2002. Stabilization mechanisms of soil organic matter: implications for C-saturation of soils. Plant and Soil 241, 155–176. https://doi.org/10.1023/a:1016125726789.
Skjemstad, J., Bushby, H., Hansen, R., 1990. Extractable Fe in the surface horizons of a range of soils from Queensland. Soil Res. 28, 259–266. https://doi.org/10.1071/sr9900259.
Slessarev, E.W., Lin, Y., Bingham, N.L., Johnson, J.E., Dai, Y., Schimel, J.P., Chadwick, O. A., 2016. Water balance creates a threshold in soil pH at the global scale. Nature 540, 567–569. https://doi.org/10.1038/nature20139.
Soil Survey Staff, 2014. Keys to Soil Taxonomy 12th edition. United States Department of Agriculture Natural Resources Conservation Service, Washington, D.C.
Sollins, P., Homann, P., Caldwell, B.A., 1996. Stabilization and destabilization of soil organic matter: mechanisms and controls. Geoderma 74, 65–105. https://doi.org/10.1016/s0016-7061(96)00036-5.
Sparks, D.L., 2003. Environmental Soil Chemistry. Elsevier. https://doi.org/10.1016/b978-0-12-656446-4.x5000-2.
Tadros, T., 2013. Ostwald ripening. In: Encyclopedia of Colloid and Interface Science, p. 820. https://doi.org/10.1007/978-3-642-20665-8_124.
Takahashi, T., Dahlgren, R.A., 2016. Nature, properties and function of aluminum–humus complexes in volcanic soils. Geoderma 263, 110–121. https://doi.org/10.1016/j.geoderma.2015.08.032.
Takahashi, T., Ikeda, Y., Fujita, K., Nanzyo, M., 2006. Effect of liming on organically complexed aluminum of nonallophanic Andosols from northeastern Japan. Geoderma 130, 26–34. https://doi.org/10.1016/j.geoderma.2005.01.006.
Takahashi, T., Kanno, H., Nanzyo, M., 2012. Factors affecting organic carbon accumulation in humus horizons of volcanic soils from the Tohoku University World Andosol Database. Pedologist 56, 58–62. https://doi.org/10.18920/pedologist.56.2_58.
Tamrat, W.Z., Rose, J., Grauby, O., Doelsch, E., Levard, C., Chaurand, P., Basile-Doelsch, I., 2019. Soil organo-mineral associations formed by co-precipitation of Fe, Si and Al in presence of organic ligands. Geochim Cosmochim Ac 260, 15–28. https://doi.org/10.1016/j.gca.2019.05.043.
Tipping, E., 2002. Cation binding by humic substances.
Tonneijck, F.H., Jansen, B., Nierop, K.G.J., Verstraten, J.M., Sevink, J., Lange, L.D., 2010. Towards understanding of carbon stocks and stabilization in volcanic ash soils in natural Andean ecosystems of northern Ecuador. Eur. J. Soil Sci. 61, 392–405. https://doi.org/10.1111/j.1365-2389.2010.01241.x.
Torn, M.S., Trumbore, S.E., Chadwick, O.A., Vitousek, P.M., Hendricks, D.M., 1997. Mineral control of soil organic carbon storage and turnover. Nature 389, 170–173. https://doi.org/10.1038/38260.
Totsche, K.U., Amelung, W., Gerzabek, M.H., Guggenberger, G., Klumpp, E., Knief, C., Lehndorff, E., Mikutta, R., Peth, S., Prechtel, A., Ray, N., Kögel-Knabner, I., 2018. Microaggregates in soils. J. Plant Nutr. Soil Sci. 181, 104–136. https://doi.org/10.1002/jpln.201600451.
Ugolini, F.C., Dahlgren, R.A., 2002. Soil Development in Volcanic Ash. Glob. Environ. Res. 6, 69–81. https://doi.org/10.57466/ger.6.2_69.
Wada, K., 1985. Advances in soil science. Adv. Soil Sci. 173–229. https://doi.org/10.1007/978-1-4612-5088-3_4.
Wada, K., Higashi, T., 1976. The categories of aluminium- and iron-humus complexes in Ando soils determined by selective dissolution. J. Soil Sci. 27, 357–368. https://doi.org/10.1111/j.1365-2389.1976.tb02007.x.
Wada, K., Kakuto, Y., 1985. Embryonic halloysites in ecuadorian soils derived from volcanic ash. Soil Sci. Soc. Am. J. 49, 1309–1318. https://doi.org/10.2136/sssaj1985.03615995004900050047x.
Wada, K., Kakuto, Y., Muchena, F.N., 1987. Clay minerals and humus complexes in five Kenyan soils derived from volcanic ash. Geoderma 39, 307–321. https://doi.org/10.1016/0016-7061(87)90050-4.
Wagai, R., Kajiura, M., Asano, M., 2020. Iron and aluminum association with microbially processed organic matter via meso-density aggregate formation across soils: organo-metallic glue hypothesis. Soil 6, 597–627. https://doi.org/10.5194/soil-6-597-2020.
Wagai, R., Mayer, L.M., 2007. Sorptive stabilization of organic matter in soils by hydrous iron oxides. Geochim. Cosmochim. Acta 71, 25–35. https://doi.org/10.1016/j.gca.2006.08.047.
Wagai, R., Mayer, L.M., Kitayama, K., Shirato, Y., 2013. Association of organic matter with iron and aluminum across a range of soils determined via selective dissolution techniques coupled with dissolved nitrogen analysis. Biogeochemistry 112, 95–109. https://doi.org/10.1007/s10533-011-9652-5.
Walkley, A., Black, I.A., 1934. An examination of the Degtjareff method for determining soil organic matter, and a proposed modification of the chromic acid titration method. Soil Sci. 37, 29–38. https://doi.org/10.1097/00010694-193401000-00003.
Watanabe, T., Harsh, J.B., Wagai, R., 2023. Short-range ordered aluminosilicates. In: Reference Module in Earth Systems and Environmental Sciences. https://doi.org/10.1016/b978-0-12-822974-3.00223-8.
Wickham, H., 2016. ggplot2, Second Edition. ed, Use R! https://doi.org/10.1007/978-3-319-24277-4.
Wiesmeier, M., Urbanski, L., Hobley, E., Lang, B., von Lützow, M., Marin-Spiotta, E., van Wesemael, B., Rabot, E., Ließ, M., Garcia-Franco, N., Wollschläger, U., Vogel, H.-J., Kögel-Knabner, I., 2019. Soil organic carbon storage as a key function of soils – a review of drivers and indicators at various scales. Geoderma 333, 149–162. https://doi.org/10.1016/j.geoderma.2018.07.026.
Wood, S., 2022. mgcv: Mixed GAM Computation Vehicle with Automatic Smoothness Estimation.
Wood, S.N., 2006. In: Generalized Additive Models: An Introduction With R. https://doi.org/10.1201/9781315370279.
Wood, S.N., 2003. Thin plate regression splines. J. R. Stat. Soc. Ser. B (Stat Methodol.) 65, 95–114. https://doi.org/10.1111/1467-9868.00374.
Yu, W., Weintraub, S.R., Hall, S.J., 2021. Climatic and geochemical controls on soil carbon at the continental scale: interactions and thresholds. Global Biogeochem Cy 35. https://doi.org/10.1029/2020gb006781.
Zieger, A., Kaiser, K., Kaupenjohann, M., 2026. Dissolved organic matter and high precipitation drive in-situ transition from silandic to aluandic properties. Geoderma 466, 117689. https://doi.org/10.1016/j.geoderma.2026.117689.